Composite Structures 377 (2026) 119883

Contents lists available at ScienceDirect

Composite Structures

journal homepage: www.elsevier.com/locate/compstruct

Nonlinear composite beam finite elements with arbitrary cross-sectional displacement fields☆

E. Carrera [a,b,1], D. Scano [a,2,*]

[a] MUL[2] Lab, Department of Mechanical and Aerospace Engineering, Politecnico di Torino, Corso Duca degli Abruzzi 24, 10129 Torino, Italy

[b] Department of Mechanical Engineering, College of Engineering, Prince Mohammad Bin Fahd University, P.O. Box 1664, Al Khobar 31952, Kingdom of Saudi Arabia

ARTICLE INFO

Keywords:
Finite element method
Composite beam models
Carrera Unified Formulation
Refined theories
Lagrange polynomials
Nonlinear analysis

ABSTRACT

This paper presents an approach to developing one-dimensional structural theories for quasi-static nonlinear analysis. This paper is developed within the beam Unified Formulation, which enables results with 3D-like accuracy. In the context of nonlinear analysis, however, it is particularly desirable to obtain accurate stress results and equilibrium curves using efficient models, as these analyses often involve complex and time-consuming procedures. Thus, the purpose of this paper is to enable each displacement component to be represented by an independent expansion function, allowing the integration of both Taylor- and Lagrange-based models within a unified framework. Moreover, the method should facilitate the combination of the Equivalent Single Layer and Layer-Wise approaches within a single structural theory. The proposed structural model is implemented within a finite element framework using a modified version of the Unified formulation, enabling the analysis of complex structures. The governing equations are derived through the principle of virtual displacements and linearized using the Newton–Raphson method. Furthermore, the Crisfield arc-length method is adopted as the incremental solution scheme. The accuracy of the proposed models is assessed by comparing displacement and stress results for composite multilayered beams with data from the literature, focusing on large-deflection and post-buckling behaviours.

1. Introduction

Nonlinear analysis is crucial for accurately predicting structural behaviour in specific configurations. This study focuses solely on geometrical nonlinearities [1], as large displacements and rotations significantly influence the accurate modelling of flexible beams [2]. Such beams remain widely used in applications like telescopes, space antennas, and robotic arms [3–5]. In particular, this paper focuses on the composite laminated structures. Fig. 1 depicts a generic multilayered beam and the reference system, that will be used in the paper. The y–direction lies along with the beam axis. Here, the cross-section (in the x-z plane), denoted as A, is subdivided into different domains k. The generic displacement field is given by the following vector:

$$\mathbf{u}^k(x,y,z) = \left\{ \begin{array}{ccc} u_x^k(x,y,z), & u_y^k(x,y,z), & u_z^k(x,y,z) \end{array} \right\}^\top \tag{1}$$

where the transposed operation is indicated by $(\cdot)^\top$.

These materials have several advantages with respect to the isotropic ones. For instance, the structures are usually much lighter, and the thermo-mechanical properties can be tailored by choosing the appropriate stacking sequence. However, composite structures are affected by complex mechanical phenomena due to their intrinsic anisotropy, such as the shear continuity between layers or the zig-zag distribution of displacements (commonly referred to as the C_z^0-requirements [6]). Also, the interactions between out-of-plane and in-plane strain components are important. Nonlinear analyses are typically computationally intensive. This work focuses on achieving two concurrent objectives: (a) maintaining accurate prediction of displacements and out-of-plane stresses while (b) implementing strategies to reduce the system's degrees of freedom for improved computational efficiency.

After having introduced the issues of the composite beams in the nonlinear regime, in this paragraph the classical are illustrated. Elastica theory [7,8], based on Euler–Bernoulli Beam Model (EBBT) [9], models

☆ This article is part of a Special issue entitled: 'Rolfes 65th' published in Composite Structures.

* Corresponding author.
E-mail addresses: erasmo.carrera@polito.it (E. Carrera), daniele.scano@polito.it (D. Scano).

1 Professor of Aeronautics and Astronautics.

2 Postdoctoral Researcher.

https://doi.org/10.1016/j.compstruct.2025.119883
Received 12 June 2025; Received in revised form 27 August 2025; Accepted 20 November 2025
Available online 21 November 2025

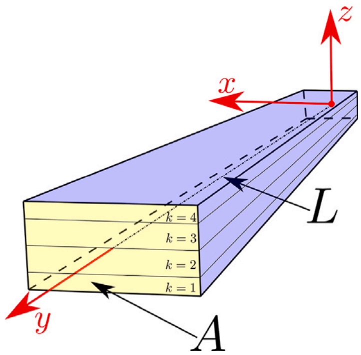

Fig. 1. Cartesian reference system for a multilayered beam structure. L is the beam axis, and A is the cross-section. k indicates the mathematical subdomain.

nonlinear flexural behaviour but is too restrictive for composites. The Timoshenko Beam Model (TBM) [10] overcomes this by including shear effects, as shown in applications like Reissner's analysis of thin curved beams [11]. Additionally, composite structures have been extensively investigated under conditions involving large displacements and rotations. Lanc et al. [12] studied the post-buckling behaviour of composite laminated beam structures in an updated Lagrangian incremental approach. This model assumed a fixed cross-section in its plane and neglected shear strains, which is consistent with the EBBM. Kurtaran [13] employed the generalized differential quadrature method for the transient analysis of curved beams. This study integrated Green–Lagrange (GL) nonlinear strain–displacement relations while adhering to the assumptions of the TBM.

Even though the classical models are convenient and relatively fast for several applications and to understand the general behaviour of the beams, more advanced theories must be introduced for studying more complex phenomena. In fact, higher-order models are crucial for the study of structures with thin-walled cross-sections and composite laminates, particularly when complicated effects, such as bending-torsion and axial-bending couplings, significantly impact their behaviour. They are also essential for achieving precise stress analysis, particularly in scenarios involving large displacements. For these reasons, a one-dimensional finite elements (FE) model was proposed by Kapania and Raciti [14] to study laminated composite beams. Obst and Kapania [15] incorporated a parabolic shear strain distribution along the transverse component while satisfying shear stress-free boundary conditions. Özütok and Madenci [16] studied the laminated structures with a FE model with ten DOFs for each node that studied the shear deformation of the cross-section. Singh et al. [17] used twelve degrees of freedom per node for constructing a refined FE to study structures with asymmetric stacking sequences. The nonlinearities of von Kármán-type are adopted in the framework. The adoption of this kind of nonlinearities can be non sufficient to describe the equilibrium curves. For this reason, the present work will adopt the complete Green–Lagrange nonlinear matrix. More information will be given in the next paragraphs. Chandrashekhara and Bangera [18] investigated the flexural behaviour by considering the shear deformation. Krawczyk et al. [19] and Krawczyk and Rebora [20] assumed first-order expansions for each material layer, in order to study the shear deformation. This paper is limited into the first-order expansion, but it would be useful to have higher-order models to describe the stresses correctly. In Vidal and Polit [21], a parabolic beam element was used with sinus structural theory for each layer. On the other hand, the C_z^0 requirements were ensured by adopting cosine-based functions for the determination of the transverse shear strain. Then, thin-walled composite beams were analysed by Mororó et al. [22] through a total Lagrangian formulation, considering large displacements and moderate rotations. Furthermore, Li and Qiao [23] employed Reddy's high-order shear deformation [24] by using the von Kármán-type assumptions for the nonlinearity in the thermal post-buckling analysis. Machado [25] investigated the post-buckling behaviour of thin-walled structures, where each displacement component was expressed using a different expansion function. Both polynomial and trigonometric terms were included. In this case, the formulation is powerful since it gives the possibility to select several types of higher-order theories. However, it is not possible to use piece-wise models. Large torsion and warping effects were studied by Mohri et al. [26] by using a finite element with seven terms for each node. Xie et al. [27] implemented a general refined zig-zag framework in aerothermoelasticity, capable of reducing to several plate models found in the literature. However, the transverse displacement follows only the classical effects. This aspect is present in several higher-order models and it is a problem, since the transverse stresses are not evaluated. They are particularly important for the free-edge analysis. Khaniki et al. [28] studied the sandwich multi-layered hyperelastic beams by adopting (a) EBBT, (b) TBM, (c) third-order theory, (d) exponential, and (e) trigonometric for the axial displacement component. The limits of this formulation are due to the fact that the other displacement component is not included and the transverse component is constant. Kim et al. [29] proposed piece-wise theories for studying beams with interlayer slips, through which complicated beams can be studied. Four- and sixteen-node cross-sectional elements are used. Adam et al. [30] studied slightly curved composite structures with Euler–Bernoulli piece-wise models. These last two examples are very powerful, however they are limited in studying moderate nonlinearities and cannot use implement all the models in a unique formulation.

The previous structural models can be divided into two modelling approaches. When accurate analyses are required, the Layer-Wise (LW) approach is often employed because it allows the assignment of distinct sets of generalized degrees of freedom to each layer (see more details in Pagani et al. [31]). The LW technique may entail a higher computational cost compared to the Equivalent Single Layer (ESL) approach, which models the multilayered structure as a single layer with homogenized properties. While ESL can reduce computational effort, it may compromise result accuracy. In particular, the LW models are needed to accurately describe the out-of-plane stresses. Usually, the adoption of ESL approach is sufficient for studying the displacements. However, this aspect is problem-dependent, and LW may be needed for obtaining optimal equilibrium curves. For all these reasons, the majority of the previous works cannot study all the aspects. One of the goals of the paper is to understand which displacement components has to use the LW approach.

Finally, in the last decade, the so-called Carrera Unified Formulation (CUF) has been used for the nonlinear behaviour of structures. In these cases, the complete Green–Lagrange (GL) matrix for the displacement-strain relationship is employed alongside a total Lagrangian approach. CUF is a versatile method for deriving beam, plate, and shell models. Within this framework, it is straightforward to select the desired expansions over the cross-section of a beam and the shape function along the structure's axis. In addition to this, both ESL and LW models can be used without changing the underlying mathematical machinery. For further details, Carrera et al. [32]. The beam assumptions were first used to create a CUF-based strong formulation in Carrera and Giunta [33]. Carrera et al. [34] analysed compact and thin-walled airfoil sections inside a FE framework with very refined *Taylor-like expansions*.

Furthermore, Carrera et al. [35] demonstrated the peculiar abilities of this formulation in studying shell-like structures. On the other hand, Lagrange-like expansions have been inserted into the CUF to study very complicated cross-sections and/or with laminated materials [36, 37]. The cross-section is represented by Lagrange Points (LP), whose interpolated displacements define the 3D field; DOFs equal the sum of displacements at all points. In the CUF literature, three Lagrange expansions are adopted, see Fig. 2. For instance, it is possible to write

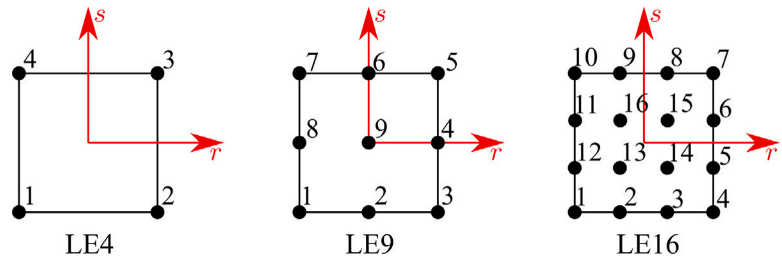

Fig. 2. Two-dimensional Lagrange expansions depicted in the natural plane. LE4: bi-linear, LE9: bi-quadratic, and LE16: bi-cubic interpolations.

in the bi-quadratic interpolation:

$$\begin{aligned} F_\tau &= \frac{1}{4}(r^2 + r r_\tau)(s^2 + s s_\tau) && \tau = 1,3,5,7 \\ F_\tau &= \frac{1}{2}s_\tau^2(s^2 - s s_\tau)(1-r^2) + \frac{1}{2}r_\tau^2(r^2 - r r_\tau)(1-s^2) && \tau = 2,4,6,8 \\ F_\tau &= (1-r^2)(1-s^2) && \tau = 9 \end{aligned} \tag{2}$$

where r and s range from -1 to $+1$, while r_τ and s_τ represent the coordinates of the LPs. A transformation is required to convert these natural coordinates into real coordinates $x - z$.

The displacement model based on the Lagrange expansion can now be formulated for a laminated structure. Specifically, quadratic interpolation functions may be employed as follows:

$$\begin{aligned} u_x^k &= F^k_{u_x1}u^k_{x_1} + F^k_{u_x2}u^k_{x_2} + F^k_{u_x3}u^k_{x_3} + F^k_{u_x4}u^k_{x_4} + F^k_{u_x5}u^k_{x_5} + F^k_{u_x6}u^k_{x_6} \\ &\quad + F^k_{u_x7}u^k_{x_7} + F^k_{u_x8}u^k_{x_8} + F^k_{u_x9}u^k_{x_9} \\ u_y^k &= F^k_{u_y1}u^k_{y_1} + F^k_{u_y2}u^k_{y_2} + F^k_{u_y3}u^k_{y_3} + F^k_{u_y4}u^k_{y_4} + F^k_{u_y5}u^k_{y_5} + F^k_{u_y6}u^k_{y_6} \\ &\quad + F^k_{u_y7}u^k_{y_7} + F^k_{u_y8}u^k_{y_8} + F^k_{u_y9}u^k_{y_9} \\ u_z^k &= F^k_{u_z1}u^k_{z_1} + F^k_{u_z2}u^k_{z_2} + F^k_{u_z3}u^k_{z_3} + F^k_{u_z4}u^k_{z_4} + F^k_{u_z5}u^k_{z_5} + F^k_{u_z6}u^k_{z_6} \\ &\quad + F^k_{u_z7}u^k_{z_7} + F^k_{u_z8}u^k_{z_8} + F^k_{u_z9}u^k_{z_9} \end{aligned} \tag{3}$$

After having used these models in the linear framework, Pagani and Carrera [38] introduced nonlinear modelling for compact and thin-walled isotropic beams, employing both Taylor- and Lagrange-based theories to analyse large deflections and post-buckling behaviour. Subsequently, they [39] extended their study to composite beams, where the use of Lagrange models enabled the accurate computation of shear stresses. Pagani et al. [40] further investigated the normal modes of isotropic beams in the nonlinear regime. The material nonlinearities have been incorporated in the CUF-based beam formulation [41], for the evaluation of soft materials. Nonlinear relationships were also incorporated into a two-dimensional (2D) plate formulation in [42], where the full GL and the classical von Kármán nonlinear models were compared. Additionally, Wu et al. [43] extended these concepts to develop a nonlinear shell formulation.

The works in this brief review have shown that it is possible to build tailored, accurate models for predicting highly complex behaviour in linear and nonlinear regimes. In these cases, when a new theory is implemented, however, the governing equations must be recalculated every time. Thus, it would be valuable to develop a general formulation that allows researchers to select different ad hoc theories, enabling them to achieve optimal results with minimal computational cost. In this case, it is useful to remember the Taylor-like expansions which are formulated in the form $x^a z^b$, where a and b are positive integers. Through the inclusion of the higher-order terms, it is possible to describe the cross-section behaviour accurately. The general expression is given

$$\begin{aligned} u_x &= u_{x_1} + x u_{x_2} + z u_{x_3} + x^2 u_{x_4} + xz u_{x_5} + z^2 u_{x_6} + \cdots + x^a z^b u_{x_N} \\ u_y &= u_{y_1} + x u_{y_2} + z u_{y_3} + x^2 u_{y_4} + xz u_{y_5} + z^2 u_{y_6} + \cdots + x^a z^b u_{y_N} \\ u_z &= u_{z_1} + x u_{z_2} + z u_{z_3} + x^2 u_{z_4} + xz u_{z_5} + z^2 u_{z_6} + \cdots + x^a z^b u_{z_N} \end{aligned} \tag{4}$$

where a and b are integers and N indicates the number of terms.

From the previous general expansions it is possible to create three types of theories, that can be summarized as follows:

- *Uniform theories:* The same expansion was applied to all three displacement variables.
- *Different theories:* It is possible to adopt distinct complete Taylor expansion for each displacement variable as well.
- *Reduced theories:* Here certain terms are deliberately omitted from the complete expansions. This omission is driven by physical considerations, as only certain terms are essential to achieve a solution that closely approximates the exact one.

Furthermore, the proposed formulation should also have the possibility to use the two approaches for different displacement components.

In recent decades, researchers have developed various methods to establish unified frameworks, enabling the selection of multiple model types. Prominent examples include the Generalized Beam Theory (GBT), introduced by Schardt [44], and the aforementioned CUF. Although the results are promising, they do not assess the individual contributions of each term in the expansion, and they cannot use diverse approaches for the different components. This work aims to develop a consistent formulation that allows users to select theories with the desired level of accuracy. Given that computational efficiency is crucial in structural analysis, achieving reliable results at minimal cost is of significant interest. In addition to this, the present study explores also the integration of ESL (for Taylor-based polynomials) and LW (for Lagrange polynomials) approaches within the same structural models, and the resulting models can be called *ESL/LW mixed theories*. The following set is a good example of this mixed approach, where Lagrange, and reduced Taylor models are used:

$$\begin{aligned} u_x^k &= F^k_{u_x1}u^k_{x_1} + F^k_{u_x2}u^k_{x_2} + F^k_{u_x3}u^k_{x_3} + F^k_{u_x4}u^k_{x_4} + F^k_{u_x5}u^k_{x_5} + F^k_{u_x6}u^k_{x_6} \\ &\quad + F^k_{u_x7}u^k_{x_7} + F^k_{u_x8}u^k_{x_8} + F^k_{u_x9}u^k_{x_9} \\ u_y &= u_{y_1} + x u_{y_2} + z u_{y_3} \\ u_z &= u_{z_1} + x u_{z_2} + z u_{z_3} + x^2 u_{z_4} + xz u_{z_5} + z^2 u_{z_6} \end{aligned} \tag{5}$$

The number of terms for the in-plane displacement u_x^k depends on the number of layers, whereas the 'ESL' terms remain fixed at three for u_y and u_z.

In conclusion, to the authors' knowledge, a unified approach for automatically generating reduced beam models in the nonlinear regime remains undeveloped. This work extends the linear framework previously investigated by Carrera and coworkers for different applications. In particular, Ref. [45] implemented a global/local approach for beam with complex sections. In [46] the importance of the are studied, while the mixed ESL/LW models are adopted for the shell formulation [47]. In these works, the Unified Formulation's capabilities for the nonlinear quasi-static analysis were significantly enhanced.

Scheme of the work. The present work follows the scheme: (a) Section 2 presents the fundamental principles of the Unified Formulation approximation and its integration into the finite element method. (b) Section 3 discusses the nonlinear beam formulation within a total Lagrangian framework, providing detailed derivations of the governing equations and FE matrices. (c) To demonstrate the new method, Section 4 presents a comprehensive example of the assembly of the tangent stiffness matrix. (d) The results concerning the accurate evaluation of displacements and stresses are showcased in Section 5. (e) Section 6 summarizes the key conclusions and outlines potential future advancements.

2. Unified formulation for beam and generalization to the higher-order theories

The Introductory section reviewed various models from the literature, and theoretically, additional *ad hoc* models can be developed. The present section presents the generalized displacement field within the FE context in the modified version of Unified formulation. A compact notation will be shown, which will be useful in deriving the governing equations.

The CUF provides a unique capability to represent all these models within a unified framework, using a consistent mathematical foundation. The expansion is formulated by introducing base functions $F^k_\tau(x,z)$, which are defined over the beam section.

The 3D displacement field is expressed as a general expansion, where each displacement component is represented using arbitrary functions defined over the domain. In addition, the FEM can be integrated in the CUF to obtain numerical solutions. Consequently:

$$\begin{aligned} u_x^k &= N_i(y)F^k_{u_x\tau}(x,z)q^k_{x_{\tau i}} \quad \text{with } \tau=1,\dots,M_{u_x} \text{ and } i=1,\dots,N_n \\ u_y^k &= N_i(y)F^k_{u_y\tau}(x,z)q^k_{y_{\tau i}} \quad \text{with } \tau=1,\dots,M_{u_y} \text{ and } i=1,\dots,N_n \\ u_z^k &= N_i(y)F^k_{u_z\tau}(x,z)q^k_{z_{\tau i}} \quad \text{with } \tau=1,\dots,M_{u_z} \text{ and } i=1,\dots,N_n \end{aligned} \tag{6}$$

$F^k_{u_x\tau}$, $F^k_{u_y\tau}$, and $F^k_{u_z\tau}$ denote the expansion functions corresponding. The Einstein's notation is used on the index τ, and M_{u_x}, M_{u_y}, and M_{u_z} identify the numbers of expansions applied. Furthermore, N_i represents the shape functions. i indicates the summation. Finally, N_n are the number of shape functions. In this formulation, it is possible to decide every type of shape function for the beam approximation. Here, the Lagrange finite elements are adopted, and more details can be found in Bathe [48].

A compact notation is chosen as described below for the sake of compactness:

$$u_l^k = N_i F^k_{u_l\tau} q^k_{l_{\tau i}} = \sum_{i=1}^{N_n}\sum_{\tau=1}^{M_{u_l}} N_i F^k_{u_l\tau} q^k_{l_{\tau i}} \tag{7}$$

$$\delta u_m^k = N_j F^k_{u_m s}\delta q^k_{m_{sj}} = \sum_{j=1}^{N_n}\sum_{s=1}^{M_{u_m}} N_j F^k_{u_m s}\delta q^k_{m_{sj}} \tag{8}$$

where l and m can take the values x, y and z. In this case, there is no summation over l (or m).

3. Nonlinear governing equations

The aim of this section is to derive the nonlinear governing equations for the specific case where only geometrical nonlinearities are present. Although the complete derivation for CUF can be found in previous papers [39], it is necessary to demonstrate that the equations for the modified version of the formulation retain the same structure. In particular, the internal and external force vectors and the tangent stiffness matrix are presented, along with a brief discussion of the Newton–Raphson linearization procedure.

Please note that the superscript k is not explicitly written in the following equations. To maintain consistency with the notation used in this paper, the type of matrix (e.g., tangent matrix) is denoted as a superscript (e.g., $\mathbf{K}^T$), rather than a subscript (e.g., $\mathbf{K}_T$), as is common in CUF literature. In this convention, the transpose operation is explicitly represented by $(\cdot)^\top$.

3.1. Preliminaries

The second Piola–Kirchhoff stresses (PK2, $\mathbf{S}$) and the Green–Lagrange strain (GL, $\mathbf{E}$) can be written in the following way, as in [49]:

$$\begin{aligned} \mathbf{S} &= \{ \sigma_{xx} \quad \sigma_{yy} \quad \sigma_{zz} \quad \sigma_{yz} \quad \sigma_{xz} \quad \sigma_{xy} \}^\top, \\ \mathbf{E} &= \{ \epsilon_{xx} \quad \epsilon_{yy} \quad \epsilon_{zz} \quad \epsilon_{xz} \quad \epsilon_{yz} \quad \epsilon_{xy} \}^\top \end{aligned} \tag{9}$$

The linear constitutive relation between the nonlinear stresses and the strains is illustrated in the following:

$$\mathbf{S} = \mathbf{C}\mathbf{E} \tag{10}$$

where the explicit expression of the material matrix $\mathbf{C}$ may be seen in the classical book of [24]. Regarding the geometrical relations, the relationship between the GL nonlinear strains and the displacements is formulated as follows:

$$\mathbf{E} = \mathbf{E}_l + \mathbf{E}_{nl} = (\mathbf{b}_l + \mathbf{b}_{nl})\mathbf{u} \tag{11}$$

where $\mathbf{b}_l$ and $\mathbf{b}_{nl}$ are the linear and nonlinear differential operators, respectively. See [39] for their expressions.

3.2. Internal and external force vectors

The principle of virtual displacements (PVD) is the first step to writing the nonlinear governing equations:

$$\delta L_{int} - \delta L_{est} = 0 \tag{12}$$

where δL_{int} represents the virtual internal energy, δL_{ext} denotes the virtual work of the external loadings. In this paper, the vector of internal forces, $\mathbf{F}^{int}$, and the vector of the external loadings, $\mathbf{p}$, are adopted:

$$\mathbf{F}^{int} - \mathbf{p} = \mathbf{0} \tag{13}$$

Fundamental nucleus of the vector of internal forces. The internal forces, $\mathbf{F}^{int}$, are obtained by using the virtual strain energy, δL_{int}, which is written as follows:

$$\delta L_{int} = \int_V \delta\mathbf{E}^\top\mathbf{S}\,\mathrm{d}V = \langle\delta\mathbf{E}^\top\mathbf{S}\rangle \tag{14}$$

where $\langle(\cdot)\rangle = \int_V(\cdot)\mathrm{d}V$.

The strain vector, $\mathbf{E}$, defined in Eq. (11), is specified with the generalized nodal unknowns $\mathbf{q}_{\tau i}$ as given below:

$$\mathbf{E} = (\mathbf{B}^l_{\tau i} + \mathbf{B}^{nl}_{\tau i})\mathbf{q}_{\tau i} \tag{15}$$

The matrices $\mathbf{B}^l_{\tau i}$ and $\mathbf{B}^{nl}_{\tau i}$ are described in the followings:

$$\mathbf{B}^l_{\tau i} = \begin{bmatrix} F_{u_x\tau,_x}N_i & 0 & 0 \\ 0 & F_{u_y\tau}N_{i,_y} & 0 \\ 0 & 0 & F_{u_z\tau,_z}N_i \\ F_{u_x\tau,_z}N_i & 0 & F_{u_z\tau,_x}N_i \\ 0 & F_{u_y\tau,_z}N_i & F_{u_z\tau}N_{i,_y} \\ F_{u_x\tau}N_{i,_y} & F_{u_y\tau,_x}N_i & 0 \end{bmatrix} \tag{16}$$

and

$$\mathbf{B}^{nl}_{\tau i} = \frac{1}{2} \times \begin{bmatrix} u_{x,_x}F_{u_x\tau,_x}N_i & u_{y,_x}F_{u_y\tau,_x}N_i & u_{z,_x}F_{u_z\tau,_x}N_i \\ u_{x,_y}F_{u_x\tau}N_{i,_y} & u_{y,_y}F_{u_y\tau}N_{i,_y} & u_{z,_y}F_{u_z\tau}N_{i,_y} \\ u_{x,_z}F_{u_x\tau,_z}N_i & u_{y,_z}F_{u_y\tau,_z}N_i & u_{z,_z}F_{u_z\tau,_z}N_i \\ u_{x,_x}F_{u_x\tau,_z}N_i + u_{x,_z}F_{u_x\tau,_x}N_i & u_{y,_x}F_{u_y\tau,_z}N_i + u_{y,_z}F_{u_y\tau,_x}N_i & u_{z,_x}F_{u_z\tau,_z}N_i + u_{z,_z}F_{u_z\tau,_x}N_i \\ u_{x,_y}F_{u_x\tau,_z}N_i + u_{x,_z}F_{u_x\tau}N_{i,_y} & u_{y,_y}F_{u_y\tau,_z}N_i + u_{y,_z}F_{u_y\tau}N_{i,_y} & u_{z,_y}F_{u_z\tau,_z}N_i + u_{z,_z}F_{u_z\tau}N_{i,_y} \\ u_{x,_x}F_{u_x\tau}N_{i,_y} + u_{x,_y}F_{u_x\tau,_x}N_i & u_{y,_x}F_{u_y\tau}N_{i,_y} + u_{y,_y}F_{u_y\tau,_x}N_i & u_{z,_x}F_{u_z\tau}N_{i,_y} + u_{z,_y}F_{u_z\tau,_x}N_i \end{bmatrix} \tag{17}$$

On the other hand, the virtual variation of $\mathbf{E}$ is described in terms by using the virtual variations of nodal unknowns as follows:

$$\delta\mathbf{E} = \delta\left(\left(\mathbf{B}^{l}_{sj} + \mathbf{B}^{nl}_{sj}\right)\mathbf{q}_{sj}\right) = \left(\mathbf{B}^{l}_{sj} + 2\mathbf{B}^{nl}_{sj}\right)\delta\mathbf{q}_{sj} \tag{18}$$

thus:

$$\delta\mathbf{E}^{\top} = \delta\mathbf{q}^{\top}_{sj}\left(\mathbf{B}^{l}_{sj} + 2\mathbf{B}^{nl}_{sj}\right)^{\top} \tag{19}$$

The internal energy is obtained in the followings:

$$\begin{aligned}\delta L_{int} =& \langle\delta\mathbf{E}^{\top}\mathbf{S}\rangle = \langle\delta\mathbf{q}^{\top}_{sj}\left(\mathbf{B}^{l}_{sj} + 2\mathbf{B}^{nl}_{sj}\right)^{\top}\mathbf{S}\rangle \\ =& \delta q_{u_x sj} F^{int}_{u_x sj} + \delta q_{u_y sj} F^{int}_{u_y sj} + \delta q_{u_z sj} F^{int}_{u_z sj}\end{aligned} \tag{20}$$

The vector of internal forces is expressed by the three fundamental nuclei:

$$\begin{aligned}F^{int}_{u_x sj} =& \langle F_{u_x s,x} N_j\left(\sigma_{xx} + \sigma_{xx}u_{x,x} + \sigma_{xy}u_{x,y} + \sigma_{xz}u_{x,z}\right)\rangle \\ &+ \langle F_{u_x s,z} N_j\left(\sigma_{xz} + \sigma_{xz}u_{x,x} + \sigma_{yz}u_{x,y} + \sigma_{zz}u_{x,z}\right)\rangle \\ &+ \langle F_{u_x s} N_{j,y}\left(\sigma_{xy} + \sigma_{xy}u_{x,x} + \sigma_{yy}u_{x,y} + \sigma_{yz}u_{x,z}\right)\rangle\end{aligned} \tag{21}$$

$$\begin{aligned}F^{int}_{u_y sj} =& \langle F_{u_y s,x} N_j\left(\sigma_{xy} + \sigma_{xx}u_{y,x} + \sigma_{xy}u_{y,y} + \sigma_{xz}u_{y,z}\right)\rangle \\ &+ \langle F_{u_y s,z} N_j\left(\sigma_{yz} + \sigma_{xz}u_{y,x} + \sigma_{yz}u_{y,y} + \sigma_{zz}u_{y,z}\right)\rangle \\ &+ \langle F_{u_y s} N_{j,y}\left(\sigma_{yy} + \sigma_{xy}u_{y,x} + \sigma_{yy}u_{y,y} + \sigma_{yz}u_{y,z}\right)\rangle\end{aligned} \tag{22}$$

$$\begin{aligned}F^{int}_{u_z sj} =& \langle F_{u_z s,x} N_j\left(\sigma_{xz} + \sigma_{xx}u_{z,x} + \sigma_{xy}u_{z,y} + \sigma_{xz}u_{z,z}\right)\rangle \\ &+ \langle F_{u_z s,z} N_j\left(\sigma_{zz} + \sigma_{xz}u_{z,x} + \sigma_{yz}u_{z,y} + \sigma_{zz}u_{z,z}\right)\rangle \\ &+ \langle F_{u_z s} N_{j,y}\left(\sigma_{yz} + \sigma_{xy}u_{z,x} + \sigma_{yy}u_{z,y} + \sigma_{yz}u_{z,z}\right)\rangle\end{aligned} \tag{23}$$

Fundamental nucleus of the vector of external forces. In this case, the virtual external work for the point loadings:

$$\delta L_{ext} = \delta\mathbf{u}^{\top}\mathbf{p} = \delta u_x p_{u_x} + \delta u_y p_{u_y} + \delta u_z p_{u_z} \tag{24}$$

The virtual variations with CUF and FEM (Eq. (8)) are used to obtain the following expression:

$$\delta L_{ext} = \delta q_{x_{sj}} N_j F_{u_x s} p_{u_x} + \delta q_{y_{sj}} N_j F_{u_y s} p_{u_y} + \delta q_{z_{sj}} N_j F_{u_z s} p_{u_z} \tag{25}$$

where:

$$\begin{aligned}p_{u_x sj} &= N_j F_{u_x s} p_{u_x} \\ p_{u_y sj} &= N_j F_{u_y s} p_{u_y} \\ p_{u_z sj} &= N_j F_{u_z s} p_{u_z}\end{aligned} \tag{26}$$

3.3. Newton–Raphson linearization of governing equations

The geometrical nonlinear FE analysis is based on the Eq. (13). It is typically solved using an incremental linearization approach. Usually, the Newton–Raphson method (i.e., the tangent method) is chosen as the numerical approach. The nonlinear problem is reformulated as an equivalent minimization problem of the residual function, as stated by Reddy [1]:

$$\boldsymbol{\varphi}_{res}(\mathbf{q} + \delta\mathbf{q}, \mathbf{p} + \delta\mathbf{p}) = \boldsymbol{\varphi}_{res}(\mathbf{p}, \mathbf{q}) + \frac{\partial\boldsymbol{\varphi}_{res}}{\partial\mathbf{q}}\delta\mathbf{q} + \frac{\partial\boldsymbol{\varphi}_{res}}{\partial\mathbf{p}}\delta\lambda\mathbf{p}_{ref} = 0 \tag{27}$$

where $\boldsymbol{\varphi}_{res}$ stands for the so-called vector of the *residual nodal forces*. In this notation, $\mathbf{q}$ indicates the array of unknowns, whereas $\mathbf{p}$ is the array of external forces. where $\frac{\partial\boldsymbol{\varphi}_{res}}{\partial\mathbf{q}} = \mathbf{K}^T$ is the *tangent stiffness matrix*, and $-\frac{\partial\boldsymbol{\varphi}_{res}}{\partial\mathbf{p}} = \mathbf{I}$. $\mathbf{I}$ indicates the unit matrix. In this method, the load changes in proportion with the reference loading vector $\mathbf{p}_{ref}$, while so that $\mathbf{p} = \lambda\mathbf{p}_{ref}$.

Thus, Eq. (27) can be reformulated as the following problem:

$$\mathbf{K}^T\delta\mathbf{q} = \delta\lambda\mathbf{p}_{ref} - \boldsymbol{\varphi}_{res} \tag{28}$$

A supplementary governing equation must be incorporated using a constraint formula $c(\delta\mathbf{q}, \delta\lambda)$, since the load-scaling parameter λ is treated as a variable, arriving to the system

$$\begin{cases}\mathbf{K}^T\delta\mathbf{q} = \delta\lambda\mathbf{p}_{ref} - \boldsymbol{\varphi}_{res} \\ c(\delta\mathbf{q}, \delta\lambda) = 0\end{cases} \tag{29}$$

This work employs the Crisfield arc-length method, i.e., a path-following approach, which considers both displacement and load variations. Detailed information on its application within the CUF framework can be found in [38].

3.4. Derivation of the tangent stiffness matrix

By linearizing the equilibrium equations [50], the FN of the tangent stiffness matrix $\mathbf{K}^T$ are obtained. Assuming conservative loading, the linearization of the virtual variation of external loads is zero, i.e., $\delta(\delta L_{est}) = 0$. Consequently, only the strain–displacement operators and stress–strain relations require linearization. The tangent matrix is formally derived by linearizing the virtual variation of the strain energy, as in the followings:

$$\begin{aligned}\delta(\delta L_{int}) =& \langle\delta(\delta\mathbf{E}^{\top}\mathbf{S})\rangle = \langle\delta\mathbf{E}^{\top}\delta\mathbf{S}\rangle + \langle\delta(\delta\mathbf{E})^{\top}\mathbf{S}\rangle \\ =& \delta q_{u_x sj}\left(K^T_{u_x u_x s\tau ji}\delta q_{u_x \tau i} + K^T_{u_x u_y s\tau ji}\delta q_{u_y \tau i} + K^T_{u_x u_z s\tau ji}\delta q_{u_z \tau i}\right) \\ &+ \delta q_{u_y sj}\left(K^T_{u_y u_x s\tau ji}\delta q_{u_x \tau i} + K^T_{u_y u_y s\tau ji}\delta q_{u_y \tau i} + K^T_{u_y u_z s\tau ji}\delta q_{u_z \tau i}\right) \\ &+ \delta q_{u_z sj}\left(K^T_{u_z u_x s\tau ji}\delta q_{u_x \tau i} + K^T_{u_z u_y s\tau ji}\delta q_{u_y \tau i} + K^T_{u_z u_z s\tau ji}\delta q_{u_z \tau i}\right)\end{aligned} \tag{30}$$

In this paper, the scalar $K^T_{u_m u_l s\tau ji}$, the nucleus of the tangent stiffness matrix, is taken as the fundamental nucleus of the tangent stiffness matrix. The components of the tangent matrix are composed by the following contributes: $K^0_{u_m u_l s\tau ji}$, $K^{T_1}_{u_m u_l s\tau ji}$, and $K^{\sigma}_{u_m u_l s\tau ji}$.

Derivation of $\langle\delta\mathbf{E}^{\top}\delta\mathbf{S}\rangle$. The first step consists on the linearization of the constitutive relation, $\mathbf{S} = \mathbf{CE}$. Since the present formulation considers only linear material properties, it is possible to write:

$$\delta\mathbf{S} = \delta(\mathbf{CE}) = \mathbf{C}\delta\mathbf{E} = \mathbf{C}\left(\mathbf{B}^{l}_{\tau i} + 2\mathbf{B}^{nl}_{\tau i}\right)\delta\mathbf{q}_{\tau i} \tag{31}$$

The contributions, $K^0_{u_m u_l s\tau ji}$ and $K^{T_1}_{u_m u_l s\tau ji}$, can be obtained from the linearized governing equations written below:

$$\begin{aligned}\langle\delta\mathbf{E}^{\top}\delta\mathbf{S}\rangle =& \delta\mathbf{q}^{\top}_{sj}\langle\left(\mathbf{B}^{sj}_{l} + 2\mathbf{B}^{sj}_{nl}\right)^{\top}\mathbf{C}\left(\mathbf{B}^{\tau i}_{l} + 2\mathbf{B}^{\tau i}_{nl}\right)\rangle\delta\mathbf{q}_{\tau i} \\ =& [\delta q_{u_x sj}\left(K^0_{u_x u_x s\tau ji}\delta q_{u_x \tau i} + K^0_{u_x u_y s\tau ji}\delta q_{u_y \tau i} + K^0_{u_x u_z s\tau ji}\delta q_{u_z \tau i}\right) \\ &+ \delta q_{u_y sj}\left(K^0_{u_y u_x s\tau ji}\delta q_{u_x \tau i} + K^0_{u_y u_y s\tau ji}\delta q_{u_y \tau i} + K^0_{u_y u_z s\tau ji}\delta q_{u_z \tau i}\right) \\ &+ \delta q_{u_z sj}\left(K^0_{u_z u_x s\tau ji}\delta q_{u_x \tau i} + K^0_{u_z u_y s\tau ji}\delta q_{u_y \tau i} + K^0_{u_z u_z s\tau ji}\delta q_{u_z \tau i}\right)] \\ &+ 2[\delta q_{u_x sj}\left(K^{lnl}_{u_x u_x s\tau ji}\delta q_{u_x \tau i} + K^{lnl}_{u_x u_y s\tau ji}\delta q_{u_y \tau i} + K^{lnl}_{u_x u_z s\tau ji}\delta q_{u_z \tau i}\right) \\ &+ \delta q_{u_y sj}\left(K^{lnl}_{u_y u_x s\tau ji}\delta q_{u_x \tau i} + K^{lnl}_{u_y u_y s\tau ji}\delta q_{u_y \tau i} + K^{lnl}_{u_y u_z s\tau ji}\delta q_{u_z \tau i}\right) \\ &+ \delta q_{u_z sj}\left(K^{lnl}_{u_z u_x s\tau ji}\delta q_{u_x \tau i} + K^{lnl}_{u_z u_y s\tau ji}\delta q_{u_y \tau i} + K^{lnl}_{u_z u_z s\tau ji}\delta q_{u_z \tau i}\right)] \\ &+ [\delta q_{u_x sj}\left(K^{nll}_{u_x u_x s\tau ji}\delta q_{u_x \tau i} + K^{nll}_{u_x u_y s\tau ji}\delta q_{u_y \tau i} + K^{nll}_{u_x u_z s\tau ji}\delta q_{u_z \tau i}\right) \\ &+ \delta q_{u_y sj}\left(K^{nll}_{u_y u_x s\tau ji}\delta q_{u_x \tau i} + K^{nll}_{u_y u_y s\tau ji}\delta q_{u_y \tau i} + K^{nll}_{u_y u_z s\tau ji}\delta q_{u_z \tau i}\right) \\ &+ \delta q_{u_z sj}\left(K^{nll}_{u_z u_x s\tau ji}\delta q_{u_x \tau i} + K^{nll}_{u_z u_y s\tau ji}\delta q_{u_y \tau i} + K^{nll}_{u_z u_z s\tau ji}\delta q_{u_z \tau i}\right)] \\ &+ 2[\delta q_{u_x sj}\left(K^{nlnl}_{u_x u_x s\tau ji}\delta q_{u_x \tau i} + K^{nlnl}_{u_x u_y s\tau ji}\delta q_{u_y \tau i} + K^{nlnl}_{u_x u_z s\tau ji}\delta q_{u_z \tau i}\right) \\ &+ \delta q_{u_y sj}\left(K^{nlnl}_{u_y u_x s\tau ji}\delta q_{u_x \tau i} + K^{nlnl}_{u_y u_y s\tau ji}\delta q_{u_y \tau i} + K^{nlnl}_{u_y u_z s\tau ji}\delta q_{u_z \tau i}\right) \\ &+ \delta q_{u_z sj}\left(K^{nlnl}_{u_z u_x s\tau ji}\delta q_{u_x \tau i} + K^{nlnl}_{u_z u_y s\tau ji}\delta q_{u_y \tau i} + K^{nlnl}_{u_z u_z s\tau ji}\delta q_{u_z \tau i}\right)] \\ =& [\delta q_{u_x sj}\left(K^0_{u_x u_x s\tau ji}\delta q_{u_x \tau i} + K^0_{u_x u_y s\tau ji}\delta q_{u_y \tau i} + K^0_{u_x u_z s\tau ji}\delta q_{u_z \tau i}\right) \\ &+ \delta q_{u_y sj}\left(K^0_{u_y u_x s\tau ji}\delta q_{u_x \tau i} + K^0_{u_y u_y s\tau ji}\delta q_{u_y \tau i} + K^0_{u_y u_z s\tau ji}\delta q_{u_z \tau i}\right)\end{aligned}$$

$$
\begin{aligned}
&+ \delta q_{u_z sj}\left(K^0_{u_z u_x s\tau ji}\delta q_{u_x \tau i} + K^0_{u_z u_y s\tau ji}\delta q_{u_y \tau i} + K^0_{u_z u_z s\tau ji}\delta q_{u_z \tau i}\right)]\\
&+ [\delta q_{u_x sj}\left(K^{T_1}_{u_x u_x s\tau ji}\delta q_{u_x \tau i} + K^{T_1}_{u_x u_y s\tau ji}\delta q_{u_y \tau i} + K^{T_1}_{u_x u_z s\tau ji}\delta q_{u_z \tau i}\right)\\
&+ \delta q_{u_y sj}\left(K^{T_1}_{u_y u_x s\tau ji}\delta q_{u_x \tau i} + K^{T_1}_{u_y u_y s\tau ji}\delta q_{u_y \tau i} + K^{T_1}_{u_y u_z s\tau ji}\delta q_{u_z \tau i}\right)\\
&+ \delta q_{u_z sj}\left(K^{T_1}_{u_z u_x s\tau ji}\delta q_{u_x \tau i} + K^{T_1}_{u_z u_y s\tau ji}\delta q_{u_y \tau i} + K^{T_1}_{u_z u_z s\tau ji}\delta q_{u_z \tau i}\right)]
\end{aligned}
\tag{32}
$$

In particular, the nine scalars $K^0_{u_m u_l s\tau ji}$ represent the linear part and are explicitly described in Appendix. On the other hand, the nonlinear contribution, $K^{T_1}_{u_m u_l s\tau ji}$, is made of three different parts, $2K^{lnl}_{u_m u_l s\tau ji}$, $K^{nll}_{u_m u_l s\tau ji}$, and $2K^{nlnl}_{u_m u_l s\tau ji}$, that will be explained later in more details.

First, $K^{nll}_{u_m u_l s\tau ji}$ indicate the components of the FN of the first-order nonlinear stiffness matrix and are written in the followings by using a compact notation:

For $l = x$:

$$
\begin{aligned}
K^{nll}_{u_m u_x s\tau ji} = &\left\langle \mathbf{u}_{,x}[m] C_{11} N_j N_i F_{u_m s,z} F_{u_x \tau,z}\right\rangle + \left\langle \mathbf{u}_{,x}[m] C_{16} N_j N_{i,y} F_{u_m s,x} F_{u_x \tau}\right\rangle\\
&+ \left\langle \mathbf{u}_{,x}[m] C_{16} N_{j,y} N_i F_{u_m s} F_{u_x \tau,x}\right\rangle + \left\langle \mathbf{u}_{,x}[m] C_{66} N_{j,y} N_{i,y} F_{u_m s} F_{u_x \tau}\right\rangle\\
&+ \left\langle \mathbf{u}_{,x}[m] C_{44} N_j N_i F_{u_m s,z} F_{u_x \tau,z}\right\rangle + \left\langle \mathbf{u}_{,y}[m] C_{16} N_j N_i F_{u_m s,x} F_{u_x \tau,x}\right\rangle\\
&+ \left\langle \mathbf{u}_{,y}[m] C_{66} N_j N_{i,y} F_{u_m s,x} F_{u_x \tau}\right\rangle + \left\langle \mathbf{u}_{,y}[m] C_{16} N_j N_i F_{u_m s,x} F_{u_x \tau,x}\right\rangle\\
&+ \left\langle \mathbf{u}_{,y}[m] C_{12} N_{j,y} N_i F_{u_m s} F_{u_x \tau,x}\right\rangle + \left\langle \mathbf{u}_{,y}[m] C_{26} N_{j,y} N_{i,y} F_{u_m s} F_{u_x \tau}\right\rangle\\
&+ \left\langle \mathbf{u}_{,y}[m] C_{45} N_j N_i F_{u_m s,z} F_{u_x \tau,z}\right\rangle + \left\langle \mathbf{u}_{,z}[m] C_{44} N_j N_i F_{u_m s,x} F_{u_x \tau,z}\right\rangle\\
&+ \left\langle \mathbf{u}_{,z}[m] C_{45} N_{j,y} N_i F_{u_m s} F_{u_x \tau,z}\right\rangle + \left\langle \mathbf{u}_{,z}[m] C_{13} N_j N_i F_{u_m s,z} F_{u_x \tau,x}\right\rangle\\
&+ \left\langle \mathbf{u}_{,z}[m] C_{36} N_j N_{i,y} F_{u_m s,z} F_{u_x \tau}\right\rangle
\end{aligned}
\tag{33}
$$

For $l = y$:

$$
\begin{aligned}
K^{nll}_{u_m u_y s\tau ji} = &\left\langle \mathbf{u}_{,x}[m] C_{16} N_j N_i F_{u_m s,x} F_{u_y \tau,x}\right\rangle + \left\langle \mathbf{u}_{,x}[m] C_{12} N_{j,y} N_i F_{u_m s,x} F_{u_y \tau}\right\rangle\\
&+ \left\langle \mathbf{u}_{,x}[m] C_{66} N_{j,y} N_i F_{u_m s} F_{u_y \tau,x}\right\rangle + \left\langle \mathbf{u}_{,x}[m] C_{26} N_{j,y} N_{i,y} F_{u_m s} F_{u_y \tau}\right\rangle\\
&+ \left\langle \mathbf{u}_{,x}[m] C_{45} N_j N_i F_{u_m s,z} F_{u_y \tau,z}\right\rangle + \left\langle \mathbf{u}_{,y}[m] C_{66} N_j N_i F_{u_m s,x} F_{u_y \tau,x}\right\rangle\\
&+ \left\langle \mathbf{u}_{,y}[m] C_{26} N_j N_{i,y} F_{u_m s,x} F_{u_y \tau}\right\rangle + \left\langle \mathbf{u}_{,y}[m] C_{26} N_{j,y} N_i F_{u_m s} F_{u_y \tau,x}\right\rangle\\
&+ \left\langle \mathbf{u}_{,y}[m] C_{22} N_{j,y} N_{i,y} F_{u_m s} F_{u_y \tau}\right\rangle + \left\langle \mathbf{u}_{,y}[m] C_{55} N_j N_i F_{u_m s,z} F_{u_y \tau,z}\right\rangle\\
&+ \left\langle \mathbf{u}_{,z}[m] C_{45} N_j N_i F_{u_m s,x} F_{u_y \tau,z}\right\rangle + \left\langle \mathbf{u}_{,z}[m] C_{55} N_{j,y} N_i F_{u_m s} F_{u_y \tau,z}\right\rangle\\
&+ \left\langle \mathbf{u}_{,z}[m] C_{36} N_j N_i F_{u_m s,z} F_{u_y \tau,x}\right\rangle + \left\langle \mathbf{u}_{,z}[m] C_{23} N_j N_{i,y} F_{u_m s,z} F_{u_y \tau}\right\rangle
\end{aligned}
\tag{34}
$$

For $l = z$:

$$
\begin{aligned}
K^{nll}_{u_m u_z s\tau ji} = &\left\langle \mathbf{u}_{,x}[m] C_{13} N_j N_i F_{u_m s,x} F_{u_z \tau,z}\right\rangle + \left\langle \mathbf{u}_{,x}[m] C_{36} N_{j,y} N_i F_{u_m s,x} F_{u_z \tau,z}\right\rangle\\
&+ \left\langle \mathbf{u}_{,x}[m] C_{44} N_j N_i F_{u_m s,z} F_{u_z \tau,x}\right\rangle + \left\langle \mathbf{u}_{,x}[m] C_{44} N_j N_{i,y} F_{u_m s,z} F_{u_z \tau}\right\rangle\\
&+ \left\langle \mathbf{u}_{,y}[m] C_{36} N_j N_i F_{u_m s,x} F_{u_z \tau,z}\right\rangle + \left\langle \mathbf{u}_{,y}[m] C_{23} N_{j,y} N_i F_{u_m s} F_{u_z \tau,z}\right\rangle\\
&+ \left\langle \mathbf{u}_{,y}[m] C_{45} N_j N_i F_{u_m s,z} F_{u_z \tau,x}\right\rangle + \left\langle \mathbf{u}_{,y}[m] C_{55} N_j N_{i,y} F_{u_m s,z} F_{u_z \tau}\right\rangle\\
&+ \left\langle \mathbf{u}_{,z}[m] C_{44} N_j N_i F_{u_m s,x} F_{u_z \tau,x}\right\rangle + \left\langle \mathbf{u}_{,z}[m] C_{45} N_j N_{i,y} F_{u_m s,x} F_{u_z \tau}\right\rangle\\
&+ \left\langle \mathbf{u}_{,z}[m] C_{45} N_{j,y} N_i F_{u_m s} F_{u_z \tau,x}\right\rangle + \left\langle \mathbf{u}_{,z}[m] C_{55} N_{j,y} N_{i,y} F_{u_m s} F_{u_z \tau}\right\rangle\\
&+ \left\langle \mathbf{u}_{,z}[m] C_{33} N_j N_i F_{u_m s,z} F_{u_z \tau,z}\right\rangle
\end{aligned}
\tag{35}
$$

In the expressions above, $\mathbf{u}_{,x}[m]$ represents the mth component of the vector $\frac{\partial \mathbf{u}}{\partial x}$; e.g., $u_{,x}[y] = u_{y,x}$. Analogously, $\mathbf{u}_{,x}[l]$ is the lth component of the vector $\frac{\partial \mathbf{u}}{\partial y}$, and so forth.

Second, the components of $K^{lnl}_{u_m u_l s\tau ji}$ can be easily derived from the FN $K^{nll}_{u_m u_l s\tau ji}$, since $K^{nll}_{u_m u_l s\tau ji} = \frac{1}{2} K^{lnl}_{u_l u_m \tau sij}$.

Third, the generic scalar FN $K^{nlnl}_{u_m u_l s\tau ji}$ of the second-order nonlinear stiffness matrix is described in the following:

$$
\begin{aligned}
2 \times K^{nlnl}_{u_m u_l s\tau ji} =\\
&\left\langle \mathbf{u}_{,x}[m]\mathbf{u}_{,x}[l] C_{11} N_j N_i F_{u_m s,x} F_{u_l \tau,x}\right\rangle + \left\langle \mathbf{u}_{,x}[m]\mathbf{u}_{,x}[l] C_{44} N_j N_i F_{u_m s,z} F_{u_l \tau,z}\right\rangle\\
&\left\langle \mathbf{u}_{,x}[m]\mathbf{u}_{,x}[l] C_{16} N_{j,y} N_i F_{u_m s} F_{u_l \tau,x}\right\rangle + \left\langle \mathbf{u}_{,x}[m]\mathbf{u}_{,x}[l] C_{66} N_j N_i F_{u_m s,x} F_{u_l \tau,z}\right\rangle\\
&\left\langle \mathbf{u}_{,x}[m]\mathbf{u}_{,x}[l] C_{44} N_j N_i F_{u_m s,z} F_{u_l \tau,z}\right\rangle + \left\langle \mathbf{u}_{,x}[m]\mathbf{u}_{,y}[l] C_{16} N_j N_i F_{u_m s,x} F_{u_l \tau,x}\right\rangle\\
&\left\langle \mathbf{u}_{,x}[m]\mathbf{u}_{,y}[l] C_{12} N_j N_{i,y} F_{u_m s,x} F_{u_l \tau}\right\rangle + \left\langle \mathbf{u}_{,x}[m]\mathbf{u}_{,y}[l] C_{66} N_{j,y} N_i F_{u_m s} F_{u_l \tau,x}\right\rangle\\
&\left\langle \mathbf{u}_{,x}[m]\mathbf{u}_{,y}[l] C_{26} N_{j,y} N_{i,y} F_{u_m s} F_{u_l \tau}\right\rangle + \left\langle \mathbf{u}_{,x}[m]\mathbf{u}_{,y}[l] C_{45} N_j N_i F_{u_m s,z} F_{u_l \tau,z}\right\rangle\\
&\left\langle \mathbf{u}_{,x}[m]\mathbf{u}_{,z}[l] C_{13} N_j N_i F_{u_m s,x} F_{u_l \tau,z}\right\rangle + \left\langle \mathbf{u}_{,x}[m]\mathbf{u}_{,z}[l] C_{36} N_{j,y} N_i F_{u_m s} F_{u_l \tau,z}\right\rangle\\
&\left\langle \mathbf{u}_{,x}[m]\mathbf{u}_{,z}[l] C_{44} N_j N_i F_{u_m s,z} F_{u_l \tau,x}\right\rangle + \left\langle \mathbf{u}_{,x}[m]\mathbf{u}_{,z}[l] C_{45} N_j N_{i,y} F_{u_m s,z} F_{u_l \tau}\right\rangle\\
&\left\langle \mathbf{u}_{,y}[m]\mathbf{u}_{,x}[l] C_{16} N_j N_i F_{u_m s,x} F_{u_l \tau,x}\right\rangle + \left\langle \mathbf{u}_{,y}[m]\mathbf{u}_{,x}[l] C_{66} N_j N_{i,y} F_{u_m s,x} F_{u_l \tau}\right\rangle\\
&\left\langle \mathbf{u}_{,y}[m]\mathbf{u}_{,x}[l] C_{12} N_{j,y} N_i F_{u_m s} F_{u_l \tau,x}\right\rangle + \left\langle \mathbf{u}_{,y}[m]\mathbf{u}_{,x}[l] C_{26} N_{j,y} N_{i,y} F_{u_m s} F_{u_l \tau}\right\rangle\\
&\left\langle \mathbf{u}_{,y}[m]\mathbf{u}_{,x}[l] C_{45} N_j N_i F_{u_m s,z} F_{u_l \tau,z}\right\rangle + \left\langle \mathbf{u}_{,y}[m]\mathbf{u}_{,y}[l] C_{66} N_j N_i F_{u_m s,x} F_{u_l \tau,x}\right\rangle\\
&\left\langle \mathbf{u}_{,y}[m]\mathbf{u}_{,y}[l] C_{26} N_j N_{i,y} F_{u_m s,x} F_{u_l \tau}\right\rangle + \left\langle \mathbf{u}_{,y}[m]\mathbf{u}_{,y}[l] C_{66} N_{j,y} N_i F_{u_m s} F_{u_l \tau,x}\right\rangle\\
&\left\langle \mathbf{u}_{,y}[m]\mathbf{u}_{,y}[l] C_{22} N_{j,y} N_{i,y} F_{u_m s} F_{u_l \tau}\right\rangle + \left\langle \mathbf{u}_{,y}[m]\mathbf{u}_{,y}[l] C_{55} N_j N_i F_{u_m s,z} F_{u_l \tau,z}\right\rangle\\
&\left\langle \mathbf{u}_{,y}[m]\mathbf{u}_{,z}[l] C_{36} N_j N_i F_{u_m s,x} F_{u_l \tau,z}\right\rangle + \left\langle \mathbf{u}_{,y}[m]\mathbf{u}_{,z}[l] C_{23} N_{j,y} N_i F_{u_m s} F_{u_l \tau,z}\right\rangle\\
&\left\langle \mathbf{u}_{,y}[m]\mathbf{u}_{,z}[l] C_{45} N_j N_i F_{u_m s,z} F_{u_l \tau,x}\right\rangle + \left\langle \mathbf{u}_{,y}[m]\mathbf{u}_{,z}[l] C_{55} N_j N_{i,y} F_{u_m s,z} F_{u_l \tau}\right\rangle\\
&\left\langle \mathbf{u}_{,z}[m]\mathbf{u}_{,x}[l] C_{44} N_j N_i F_{u_m s,x} F_{u_l \tau,z}\right\rangle + \left\langle \mathbf{u}_{,z}[m]\mathbf{u}_{,x}[l] C_{45} N_{j,y} N_i F_{u_m s} F_{u_l \tau,z}\right\rangle\\
&\left\langle \mathbf{u}_{,z}[m]\mathbf{u}_{,x}[l] C_{13} N_j N_i F_{u_m s,z} F_{u_l \tau,x}\right\rangle + \left\langle \mathbf{u}_{,z}[m]\mathbf{u}_{,x}[l] C_{36} N_j N_{i,y} F_{u_m s,z} F_{u_l \tau}\right\rangle\\
&\left\langle \mathbf{u}_{,z}[m]\mathbf{u}_{,y}[l] C_{45} N_j N_i F_{u_m s,x} F_{u_l \tau,z}\right\rangle + \left\langle \mathbf{u}_{,z}[m]\mathbf{u}_{,y}[l] C_{55} N_{j,y} N_i F_{u_m s} F_{u_l \tau,z}\right\rangle\\
&\left\langle \mathbf{u}_{,z}[m]\mathbf{u}_{,y}[l] C_{36} N_j N_i F_{u_m s,z} F_{u_l \tau,x}\right\rangle + \left\langle \mathbf{u}_{,z}[m]\mathbf{u}_{,y}[l] C_{23} N_j N_{i,y} F_{u_m s,z} F_{u_l \tau}\right\rangle\\
&\left\langle \mathbf{u}_{,z}[m]\mathbf{u}_{,z}[l] C_{44} N_j N_i F_{u_m s,x} F_{u_l \tau,x}\right\rangle + \left\langle \mathbf{u}_{,z}[m]\mathbf{u}_{,z}[l] C_{45} N_j N_{i,y} F_{u_m s,x} F_{u_l \tau}\right\rangle\\
&\left\langle \mathbf{u}_{,z}[m]\mathbf{u}_{,z}[l] C_{45} N_{j,y} N_i F_{u_m s} F_{u_l \tau,x}\right\rangle + \left\langle \mathbf{u}_{,z}[m]\mathbf{u}_{,z}[l] C_{55} N_{j,y} N_{i,y} F_{u_m s} F_{u_l \tau}\right\rangle\\
&\left\langle \mathbf{u}_{,z}[m]\mathbf{u}_{,z}[l] C_{33} N_j N_i F_{u_m s,z} F_{u_l \tau,z}\right\rangle
\end{aligned}
\tag{36}
$$

Derivation of $\langle \delta(\delta\mathbf{E})^\top \mathbf{S}\rangle$. The last contribution of the tangent stiffness matrix comes from the linearization of the nonlinear geometrical relationships. First, it is known from Crisfield [49] that:

$$
\delta(\delta\mathbf{E}) =
\left\{
\begin{array}{c}
\left(\delta u_{x,x}\right)_{\mathrm{v}}\delta u_{x,x} + \left(\delta u_{y,x}\right)_{\mathrm{v}}\delta u_{y,x} + \left(\delta u_{z,x}\right)_{\mathrm{v}}\delta u_{z,x}\\
\left(\delta u_{x,y}\right)_{\mathrm{v}}\delta u_{x,y} + \left(\delta u_{y,y}\right)_{\mathrm{v}}\delta u_{y,y} + \left(\delta u_{z,y}\right)_{\mathrm{v}}\delta u_{z,y}\\
\left(\delta u_{x,z}\right)_{\mathrm{v}}\delta u_{x,z} + \left(\delta u_{y,z}\right)_{\mathrm{v}}\delta u_{y,z} + \left(\delta u_{z,z}\right)_{\mathrm{v}}\delta u_{z,z}\\
\left[\left(\delta u_{x,x}\right)_{\mathrm{v}}\delta u_{x,z} + \delta u_{x,x}\left(\delta u_{x,z}\right)_{\mathrm{v}}\right] + \left[\left(\delta u_{y,x}\right)_{\mathrm{v}}\delta u_{y,z} + \delta u_{y,x}\left(\delta u_{y,z}\right)_{\mathrm{v}}\right]\\
+\left[\left(\delta u_{z,x}\right)_{\mathrm{v}}\delta u_{z,z} + \delta u_{z,x}\left(\delta u_{z,z}\right)_{\mathrm{v}}\right]\\
\left[\left(\delta u_{x,y}\right)_{\mathrm{v}}\delta u_{x,z} + \delta u_{x,y}\left(\delta u_{x,z}\right)_{\mathrm{v}}\right] + \left[\left(\delta u_{y,y}\right)_{\mathrm{v}}\delta u_{y,z} + \delta u_{y,y}\left(\delta u_{y,z}\right)_{\mathrm{v}}\right]\\
+\left[\left(\delta u_{z,y}\right)_{\mathrm{v}}\delta u_{z,z} + \delta u_{z,y}\left(\delta u_{z,z}\right)_{\mathrm{v}}\right]\\
\left[\left(\delta u_{x,x}\right)_{\mathrm{v}}\delta u_{x,y} + \delta u_{x,x}\left(\delta u_{x,y}\right)_{\mathrm{v}}\right] + \left[\left(\delta u_{y,x}\right)_{\mathrm{v}}\delta u_{y,y} + \delta u_{y,x}\left(\delta u_{y,y}\right)_{\mathrm{v}}\right]\\
+\left[\left(\delta u_{z,x}\right)_{\mathrm{v}}\delta u_{z,y} + \delta u_{z,x}\left(\delta u_{z,y}\right)_{\mathrm{v}}\right]
\end{array}
\right\}
\tag{37}
$$

the variation is indicated by the subscript "v". The CUF notation is introduced for both the linearized variables (i.e., $\delta u_l = N_i F_{u_l \tau}\delta q_{u_l \tau i}$) and the virtual variables (i.e., $(\delta u_m)_{\mathrm{v}} = N_j F_{u_m s}\delta q_{u_m sj}$), and the following expression is used:

$$
\delta(\delta\mathbf{E}) = \mathbf{B}^{nl*}
\left\{
\begin{array}{c}
\delta q_{x_{sj}}\delta q_{x_{\tau i}}\\
\delta q_{y_{sj}}\delta q_{y_{\tau i}}\\
\delta q_{z_{sj}}\delta q_{z_{\tau i}}
\end{array}
\right\}
\tag{38}
$$

$$\mathbf{B}^{nl*} = \begin{bmatrix} F_{u_x\tau,x}F_{u_xs,x}N_iN_j & F_{u_y\tau,x}F_{u_ys,x}N_iN_j & F_{u_z\tau,x}F_{u_zs,x}N_iN_j \\ F_{u_x\tau}F_{u_xs}N_{i,y}N_{j,y} & F_{u_y\tau}F_{u_ys}N_{i,y}N_{j,y} & F_{u_z\tau}F_{u_zs}N_{i,y}N_{j,y} \\ F_{u_x\tau,z}F_{u_xs,z}N_iN_j & F_{u_y\tau,z}F_{u_ys,z}N_iN_j & F_{u_z\tau,z}F_{u_zs,z}N_iN_j \\ F_{u_x\tau,x}F_{u_xs,z}N_iN_j + F_{u_x\tau,z}F_{u_xs,x}N_iN_j & F_{u_y\tau,x}F_{u_ys,z}N_iN_j + F_{u_y\tau,z}F_{u_ys,x}N_iN_j & F_{u_z\tau,x}F_{u_zs,z}N_iN_j + F_{u_z\tau,z}F_{u_zs,x}N_iN_j \\ F_{u_x\tau,z}F_{u_xs}N_iN_{j,y} + F_{u_x\tau}F_{u_xs,z}N_{i,y}N_j & F_{u_y\tau,z}F_{u_ys}N_iN_{j,y} + F_{u_y\tau}F_{u_ys,z}N_{i,y}N_j & F_{u_z\tau,z}F_{u_zs}N_iN_{j,y} + F_{u_z\tau}F_{u_zs,z}N_{i,y}N_j \\ F_{u_x\tau,x}F_{u_xs}N_iN_{j,y} + F_{u_x\tau}F_{u_xs,x}N_{i,y}N_j & F_{u_y\tau,x}F_{u_ys}N_iN_{j,y} + F_{u_y\tau}F_{u_ys,x}N_{i,y}N_j & F_{u_z\tau,x}F_{u_zs}N_iN_{j,y} + F_{u_z\tau}F_{u_zs,x}N_{i,y}N_j \end{bmatrix} \quad (40)$$

Box I.

The transpose array is written below:

$$\delta(\delta\mathbf{E})^\top = \left\{ \begin{array}{c} \delta q_{x_{sj}}\delta q_{x_{\tau i}} \\ \delta q_{y_{sj}}\delta q_{y_{\tau i}} \\ \delta q_{z_{sj}}\delta q_{z_{\tau i}} \end{array} \right\}^\top \left(\mathbf{B}^{nl*}\right)^\top \quad (39)$$

where (see Box I).

From the previous considerations, it is straightforward to study the nonlinear geometrical contribute:

$$\langle\delta(\delta\mathbf{E})^\top\mathbf{S}\rangle =< \left\{ \begin{array}{c} \delta q_{x_{sj}}\delta q_{x_{\tau i}} \\ \delta q_{y_{sj}}\delta q_{y_{\tau i}} \\ \delta q_{z_{sj}}\delta q_{z_{\tau i}} \end{array} \right\}^\top \left(\mathbf{B}^{nl*}\right)^\top \mathbf{S} > \quad (41)$$

$$\begin{aligned} \langle\delta(\delta\mathbf{E})^\top\mathbf{S}\rangle &= \delta\mathbf{q}_{sj}^\top\langle\text{diag}\left(\left(\mathbf{B}^{nl*}\right)^\top\mathbf{S}\right)\rangle\delta\mathbf{q}_{\tau i} \\ &= \delta\mathbf{q}_{sj}^\top\langle\text{diag}\left(\left(\mathbf{B}^{nl*}\right)^\top(\mathbf{S}_l+\mathbf{S}_{nl})\right)\rangle\delta\mathbf{q}_{\tau i} \\ &= \delta q_{u_xsj}\left(K^{\sigma_l}_{u_xu_xs\tau ji} + K^{\sigma_{nl}}_{u_xu_xs\tau ji}\right)\delta q_{u_x\tau i} \\ &+\delta q_{u_ysj}\left(K^{\sigma_l}_{u_yu_ys\tau ji} + K^{\sigma_{nl}}_{u_yu_ys\tau ji}\right)\delta q_{u_y\tau i} \\ &+\delta q_{u_zsj}\left(K^{\sigma_l}_{u_zu_zs\tau ji} + K^{\sigma_{nl}}_{u_zu_zs\tau ji}\right)\delta q_{u_z\tau i} \\ &= \delta q_{u_xsj}K^{\sigma}_{u_xu_xs\tau ji}\delta q_{u_x\tau i} + \delta q_{u_ysj}K^{\sigma}_{u_yu_ys\tau ji}\delta q_{u_y\tau i} + \delta q_{u_zsj}K^{\sigma}_{u_zu_zs\tau ji}\delta q_{u_z\tau i} \end{aligned} \quad (42)$$

The preceding equations illustrate the nonlinear contribution to the tangent stiffness, which is therefore referred to as *geometrical stiffness*. This stiffness consists of both a linear component, given by $\mathbf{S}_l = \mathbf{C}\mathbf{E}_l$, and a nonlinear component, given by $\mathbf{S}_{nl} = \mathbf{C}\mathbf{E}_{nl}$. Consequently, the complete fundamental nucleus is expressed as: $K^{\sigma}_{u_mu_ls\tau ji} = K^{\sigma_l}_{u_mu_ls\tau ji} + K^{\sigma_{nl}}_{u_mu_ls\tau ji}$.

The only three nonzero scalar FNs $K^{\sigma}_{u_mu_ls\tau ji}$ are explicitly given as follows:

$$\begin{aligned} K^{\sigma}_{u_xu_xs\tau ji} =& \langle\sigma_{xx}F_{u_x\tau,x}F_{u_xs,x}N_iN_j\rangle + \langle\sigma_{yy}F_{u_x\tau}F_{u_xs}N_{i,y}N_{j,y}\rangle \\ &+ \langle\sigma_{zz}F_{u_x\tau,z}F_{u_xs,z}N_iN_j\rangle + \langle\sigma_{xy}F_{u_x\tau,x}F_{u_xs}N_iN_{j,y}\rangle \\ &+ \langle\sigma_{xy}F_{u_x\tau}F_{u_xs,x}N_iN_{j,y}\rangle + \langle\sigma_{xz}F_{u_x\tau,x}F_{u_xs,z}N_iN_j\rangle \\ &+ \langle\sigma_{xz}F_{u_x\tau,z}F_{u_xs,x}N_iN_j\rangle + \langle\sigma_{yz}F_{u_x\tau,z}F_{u_xs}N_iN_{j,y}\rangle \\ &+ \langle\sigma_{yz}F_{u_x\tau}F_{u_xs,z}N_iN_j\rangle \end{aligned} \quad (43)$$

$$\begin{aligned} K^{\sigma}_{u_yu_ys\tau ji} =& \langle\sigma_{xx}F_{u_y\tau,x}F_{u_ys,x}N_iN_j\rangle + \langle\sigma_{yy}F_{u_y\tau}F_{u_ys}N_{i,y}N_{j,y}\rangle \\ &+ \langle\sigma_{zz}F_{u_y\tau,z}F_{u_ys,z}N_iN_j\rangle + \langle\sigma_{xy}F_{u_y\tau,x}F_{u_ys}N_iN_{j,y}\rangle \\ &+ \langle\sigma_{xy}F_{u_y\tau}F_{u_ys,x}N_iN_{j,y}\rangle + \langle\sigma_{xz}F_{u_y\tau,x}F_{u_ys,z}N_iN_j\rangle \\ &+ \langle\sigma_{xz}F_{u_y\tau,z}F_{u_ys,x}N_iN_j\rangle + \langle\sigma_{yz}F_{u_y\tau,z}F_{u_ys}N_iN_{j,y}\rangle \\ &+ \langle\sigma_{yz}F_{u_y\tau}F_{u_ys,z}N_iN_j\rangle \end{aligned} \quad (44)$$

$$\begin{aligned} K^{\sigma}_{u_zu_zs\tau ji} =& \langle\sigma_{xx}F_{u_z\tau,x}F_{u_zs,x}N_iN_j\rangle + \langle\sigma_{yy}F_{u_z\tau}F_{u_zs}N_{i,y}N_{j,y}\rangle \\ &+ \langle\sigma_{zz}F_{u_z\tau,z}F_{u_zs,z}N_iN_j\rangle + \langle\sigma_{xy}F_{u_z\tau,x}F_{u_zs}N_iN_{j,y}\rangle \\ &+ \langle\sigma_{xy}F_{u_z\tau}F_{u_zs,x}N_iN_{j,y}\rangle + \langle\sigma_{xz}F_{u_z\tau,x}F_{u_zs,z}N_iN_j\rangle \\ &+ \langle\sigma_{xz}F_{u_z\tau,z}F_{u_zs,x}N_iN_j\rangle + \langle\sigma_{yz}F_{u_z\tau,z}F_{u_zs}N_iN_{j,y}\rangle \\ &+ \langle\sigma_{yz}F_{u_z\tau}F_{u_zs,z}N_iN_j\rangle \end{aligned} \quad (45)$$

In this way, the FNs of the tangent stiffness matrix are expressed as the sum of all the contributions previously calculated:

$$K^T_{u_mu_ls\tau ji} = K^0_{u_mu_ls\tau ji} + K^{T_1}_{u_mu_ls\tau ji} + K^{\sigma}_{u_mu_ls\tau ji} \quad (46)$$

At this stage, the tangent stiffness matrix can be assembled. The general assembly for the CUF can be seen in [45,46] for the beam and plate formulations in the case of linear analysis.

4. Assembly

The previous section presented the mathematical framework of the proposed formulation. An equally important aspect concerns the assembly of the finite element matrices. In this section, a simple example is provided to clarify the procedure, while a more detailed explanation can be found in [46] for the linear case.

In Fig. 3, a single two-node beam element (B2) is taken into account. In the same figure, the three expansions and the respective number of terms, M_{u_l}, are illustrated. As can be seen, both u_x and u_y follow a second-order Taylor expansion model (TE2), whereas the transverse displacement, u_z, adopts the first-order model (TE1). In this way, each node has 15 degrees of freedom, and the entire structure is studied by 30 degrees of freedom. For the sake of brevity, only ESL models are shown, but it is possible to introduce LW theories as well.

Fig. 4 presents the global tangent stiffness matrix, $\mathbf{K}^T$, with dimensions of 30 × 30. Each submatrix $\mathbf{K}^T_{ji}$ is decomposed into nine submatrices, $\mathbf{K}^T_{u_mu_lij}$. For example, Fig. 5 explicitly shows the nine components of $\mathbf{K}^T_{11}$, see the circled matrices. From the scheme, it is clear that the dimensions and shapes of the matrices $\mathbf{K}^T_{u_mu_l11}$ may change according to the number of terms for each displacement component. For example, $\mathbf{K}^T_{u_xu_y11}$, is a square 6 × 6 sub-matrix since both components utilize the TE2 model. When different values of M_{u_l} (and M_{u_m}) are assigned to different components, the resulting $\mathbf{K}^T_{u_mu_l11}$ become rectangular with varying dimensions. Examples of such cases include $\mathbf{K}^T_{u_xu_z11}$, or $\mathbf{K}^T_{u_zu_y11}$. For clarity, the submatrices $\mathbf{K}^T_{u_mu_l11}$ are referred as $\mathbf{K}^T_{u_mu_l}$. In summary, each 1 × 1 $K^T_{u_mu_ls\tau ji}$ FN represents the prime components of the matrices.

The entire procedure can likewise be applied to the arrays of internal and external loads, with the distinction that only a single dimension is considered.

5. Numerical results

The main purpose of the section is to demonstrate the potentialities of the proposed methods. This section analyses two benchmark cases, assessing both displacements and stresses. The first scenario focuses on a compact square cross-section in the postbuckling behaviour, while the second investigates a two-layered beam subjected to bending.

$$\text{TE2:}\quad u_x = u_{x_1} + x u_{x_2} + z u_{x_3} + x^2 u_{x_4} + xz u_{x_5} + z^2 u_{x_6} \qquad M_{u_x} = 6$$
$$\text{TE2:}\quad u_y = u_{y_1} + x u_{y_2} + z u_{y_3} + x^2 u_{y_4} + xz u_{y_5} + z^2 u_{y_6} \qquad M_{u_y} = 6$$
$$\text{TE1:}\quad u_z = u_{z_1} + x u_{z_2} + z u_{z_3} \qquad M_{u_z} = 3$$

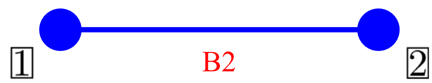

Fig. 3. Example of a linear beam element. u_x and u_y are studied by using a Taylor-based second-order model (TE2), whereas a linear theory (TE1) approximates the variable u_z.

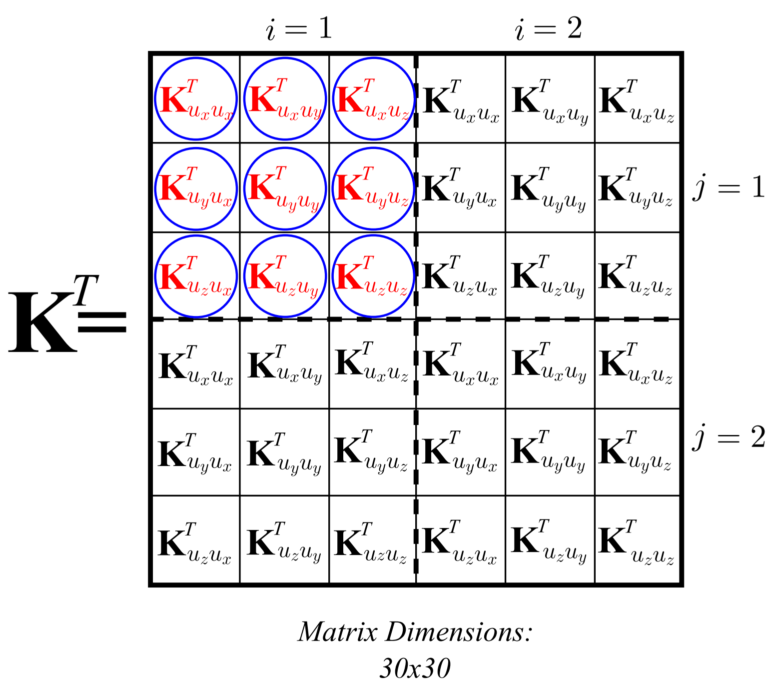

Fig. 4. Assembly of the general tangent stiffness matrix, see Fig. 3. The red sub-matrices will be considered in Fig. 5.

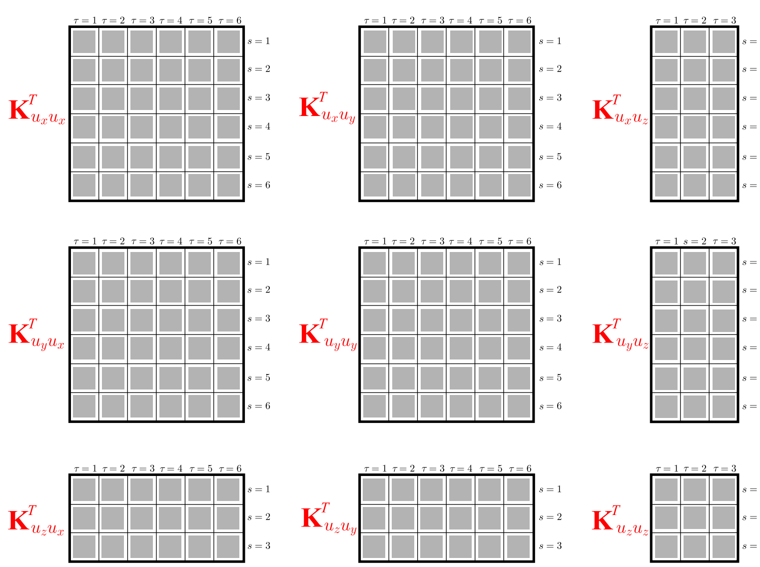

Fig. 5. Assembly of the tangent stiffness matrix (here only the submatrix $\mathbf{K}^T_{11}$ is considered).

A consistent acronym system is used to describe the structural theories. The Taylor-based expansions are described in the following way: TEn_{u_x}-TEn_{u_y}-TEn_{u_z}, where n_{u_l} denotes the polynomial order for the displacement components. For Lagrange-based expansions, the acronym

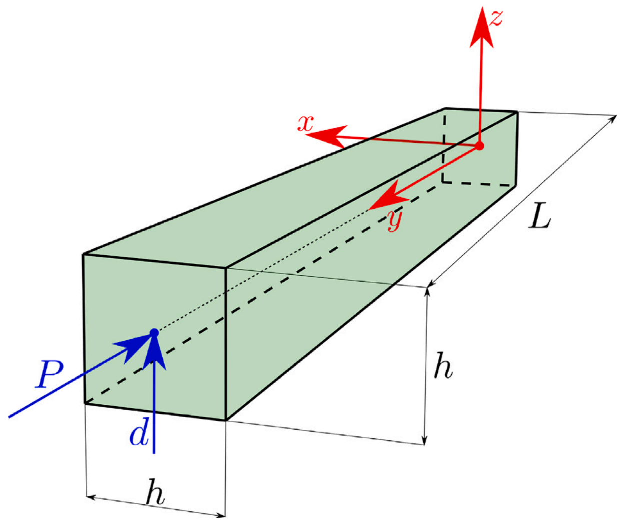

Fig. 6. Geometrical properties of a compact square beam with length-to-height ratio, $L/h = 100$. The compressive P and defect loads d are applied at the tip. The benchmark is taken from [38].

Table 1
Postbuckling analysis of a square compact beam. Details of the structural models: types of expansions, the number of terms, and DOF.

Expansions			$M_{u_x}/M_{u_y}/M_{u_z}$	DOF
u_x	u_y	u_z		
		Reference solution [38]		
LE9	LE9	LE9	9/9/9	1647
		LE/TE Models		
TE1	LE9	LE9	3/9/9	1281
TE1	LE9	TE1	3/9/3	915
const	LE9	LE9	1/9/9	1159
0	LE9	LE9	0/9/9	1098

LEp-LEp-LEp is used, where p represents the number of Lagrange points (LPs) in the CUF elements of the cross-section. The text will explicitly state the number of Lagrange CUF elements employed for each material layer. Additionally, mixed ESL/LW theories are applied, allowing for refined models such as LE16-TE3-TE2. Sometimes, a displacement component may be completely disregarded and a '0' indicates this particular condition.

5.1. Postbuckling analysis of a compact square beam

This preliminary benchmark is taken from Carrera et al. [38] and examines the geometrically non-linear behaviour of a compact square beam. Fig. 6 illustrates the geometry of the structure. The length-to-height ratio, L/h, is set at 100. The structure comprises an isotropic, aluminium-like material having the properties $E = 75$ [GPa] and $\nu = 0.33$. Regarding boundary conditions, the beam is fully clamped at the section $y = 0$. A compressive load, P, is applied at the beam tip. In order to impose a preferential solution branch, a small defect load d is applied toward the positive z-axis, see Fig. 6. The defect can be calculated according to the following expression:

$$\frac{4\ L^2}{\pi^2\ E\ I} = 0.002 \tag{47}$$

where $I = h^4/12$ stands for the second moment area for a square cross-section. Along the beam axis, twenty cubic Lagrange beam elements are implemented. The axial (u_y) and out-of-plane displacements (u_z) are computed at the distal end, located at coordinates $[0, L, 0]$.

Table 1 summarizes the kinematic theories implemented in this study. For each displacement component, two features are presented:

Table 2
Cantilevered two-layered beam under a constant bending pressure. Details of the structural models: types of expansions, the number of terms, and DOF.

Expansions			$M_{u_x}/M_{u_y}/M_{u_z}$	DOF
u_x	u_y	u_z		
		Reference solutions [39]		
LE16	LE16	LE16	28/28/28	5124
3D-ABAQUS			—	573 675
		Uniform models		
TE2	TE2	TE2	6/6/6	1098
TE3	TE3	TE3	10/10/10	1830
		ESL/LW Models		
TE2	LE16	TE2	6/28/6	2440
TE2	LE16	TE3	6/28/10	2684
TE2	LE16	TE4	6/28/15	2989
TE2	LE16	LE16	6/28/28	3782
0	LE16	LE16	0/28/28	3416
0	LE16	TE2	0/28/6	2074
TE2	TE2	LE16	6/6/28	2440

(a) the specific expansion used, and (b) the corresponding number of terms (M_{u_l}). The table first illustrates the reference LE9-LE9-LE9 solution. Subsequent rows detail the characteristics of various mixed TE/LE expansions. In this case, it is not possible to use the denominations ESL and LW, since an isotropic structure is considered. This example allows to preliminary explore the capabilities of the new method and how it is possible to adopt different assumptions for the three displacement components. In model const-LE9-LE9, 'const' means that only the constant term is employed for the displacement component u_x.

Fig. 7 illustrates the equilibrium curves for this benchmark with a comparison with the reference complete LE9-LE9-LE9 model. In particular, the non-dimensional axial and transverse displacements are shown in Figs. 7(a) and 7(b), respectively. Also, the load is given in the graph as a non-dimensional parameter: $P\ 4\ L^2/(\pi^2\ E\ I)$.

Computational costs. In this paragraph, the computational times has been investigated. In particular, the left-most part of Fig. 8 compares all the details, i.e., the DOFs, the computational times. Furthermore, the label "Convergence" indicates whether the model successfully reaches convergence. In this benchmark, only the TE1-LE9-TE1 model fails to approach the correct trend. On the right-hand of Fig. 8, the graph of the adimensionalized computational time depending on the degrees of freedom is plotted. The time is normalized respect to the reference model LE9-LE9-LE9.

The numerical results lead to the following key conclusions:

- Regarding equilibrium curves computation, almost all the reduced models follow the reference solution trend with minor discrepancies. The reduced models clearly identifies the postbuckling behaviour for both the axial and transverse displacements. In particular, the snap-back for the out-of-plane displacements is well-characterized also by the proposed models. TE1-LE9-TE1 is the least accurate model, as it entirely fails to capture the reference trends. Specifically, Fig. 7(a) clearly shows that the axial displacement remains zero.
- These analyses demonstrate how the u_x displacement component can be completely disregarded without compromising accuracy. In contrast, u_y and u_z components have a significant influence and bi-parabolic expansions must be adopted.
- The comparison of the computational costs demonstrates that the reduced models are particularly efficient. Within this group of models, 0-LE9-LE9 (with 1159 DOF, and a normalized time of 0.54) emerges as the most computationally efficient for this specific evaluation, achieving an optimal balance between accuracy and efficiency. On the other hand, TE1-LE9-TE1 has both low DOF and computational costs, but it does not reach the convergence.

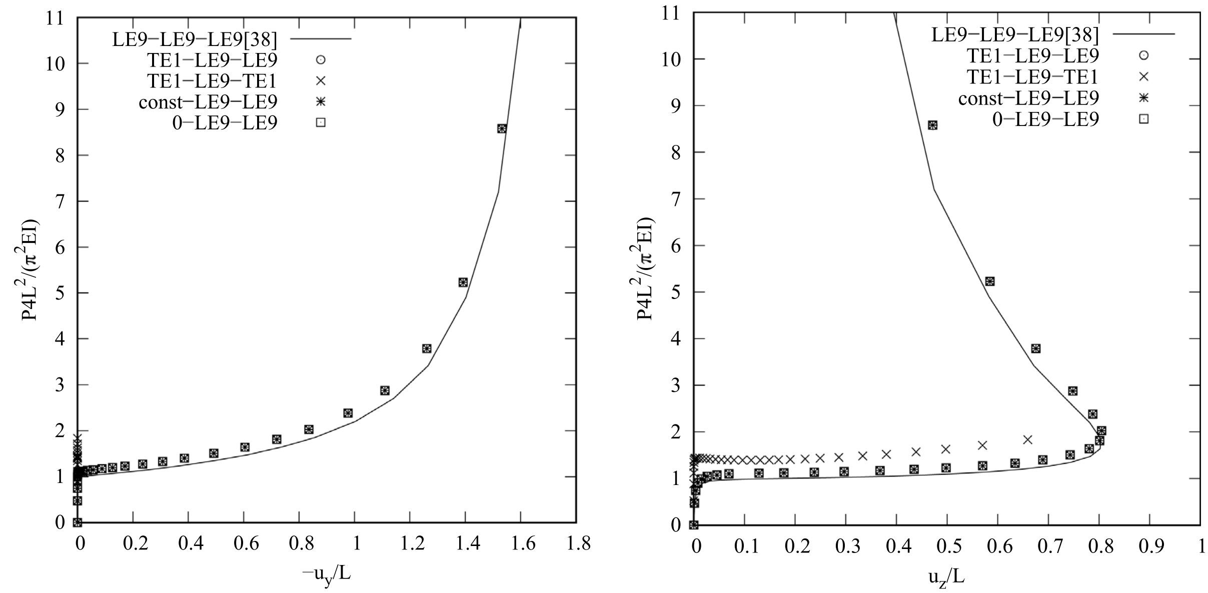

(a) Axial displacements (b) Transverse displacements

Fig. 7. Postbuckling analysis of a square compact beam. The displacements are on the horizontal axis; while the load is on the vertical axis. Equilibrium curves for the reference and the present models.

Expansions					
u_x	u_y	u_z	DOF	Time [s]	Convergence
LE9	LE9	LE9	1647	250.6	Yes
TE1	LE9	LE9	1281	156.2	Yes
TE1	LE9	TE1	915	134.6	No
const	LE9	LE9	1159	148.7	Yes
0	LE9	LE9	1098	134.4	Yes

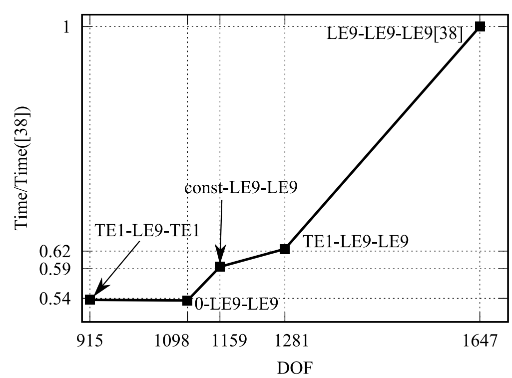

Fig. 8. Details for the computational costs. (Left) Information for the five models, and (Right) plot of the adimensionalized computational time depending the degrees of freedom.

5.2. Large deflection of a two-layered beam subjected to bending

This case study, taken from Pagani and Carrera [39], investigates the large displacement behaviour of an asymmetric multi-layered structure which presents the stacking sequence: [0°/90°]. Fig. 9 displays the geometrical properties. The structure has a length of L of 9 [m], and a section width of b = 1 [m], while the total height is h = 0.6 [m]. The two layers are composed of an orthotropic AS4/3501-06 graphite/epoxy material with the following properties: $E_L = 144.8$ [GPa], $E_2 = E_T = E_z = 9.65$ [GPa], $\nu_{LT} = \nu_{Lz} = \nu_{zT} = 0.3$, $G_{LT} = G_{Lz} = 4.14$ [GPa], and $G_{Tz} = 3.45$ [GPa]. As far as the boundary conditions are concerned, the section $y = 0$ is clamped, and a constant pressure p_0 acts in the positive z direction. Two reference models are used: (a) the CUF-base two-element LE16 expansion, and (b) a refined solid 3D-ABAQUS, both taken from [39]. Ten four-node Lagrange beam elements are employed for the y-axis. The dimensionless out-of-plane displacements, $\bar{u}_z = u_z/h$, are evaluated at the tip $[0, L, 0]$. On the contrary, the shear stresses, $\bar{\sigma}_{yz} = \sigma_{yz}/p_0$, are calculated at the mid-span of the beam $[0, L/2, z]$.

Table 2 presents the theories adopted in the current analyses. The expansions for each displacement component are shown, along with

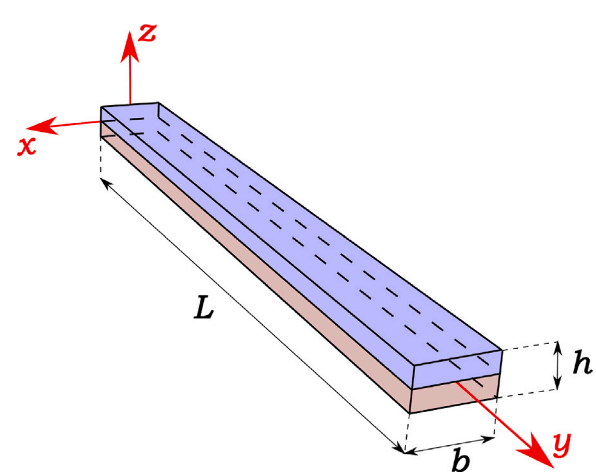

Fig. 9. Geometrical properties of an asymmetric laminated beam subjected to large bending deflections. The benchmark is taken from [39].

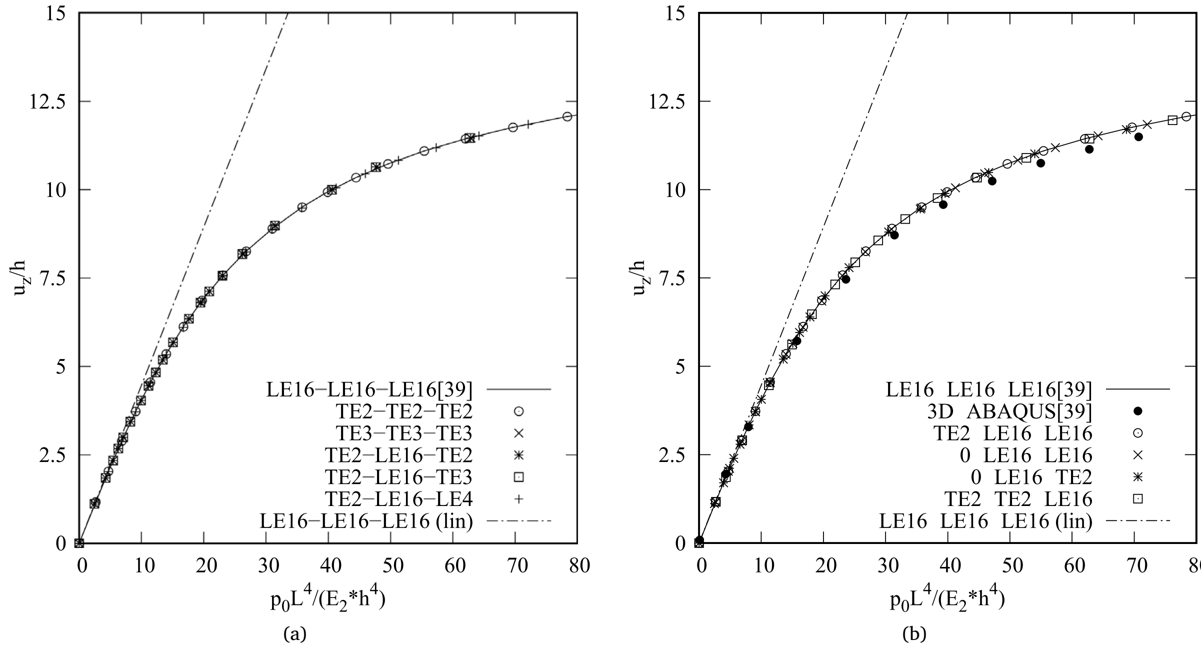

Fig. 10. Two-layer cross-ply beam subjected to bending. Linear and nonlinear equilibrium curves. The non dimensional displacements are on the vertical axis; while the non-dimensional load is on the horizontal axis. Equilibrium curves for the reference and the present models.

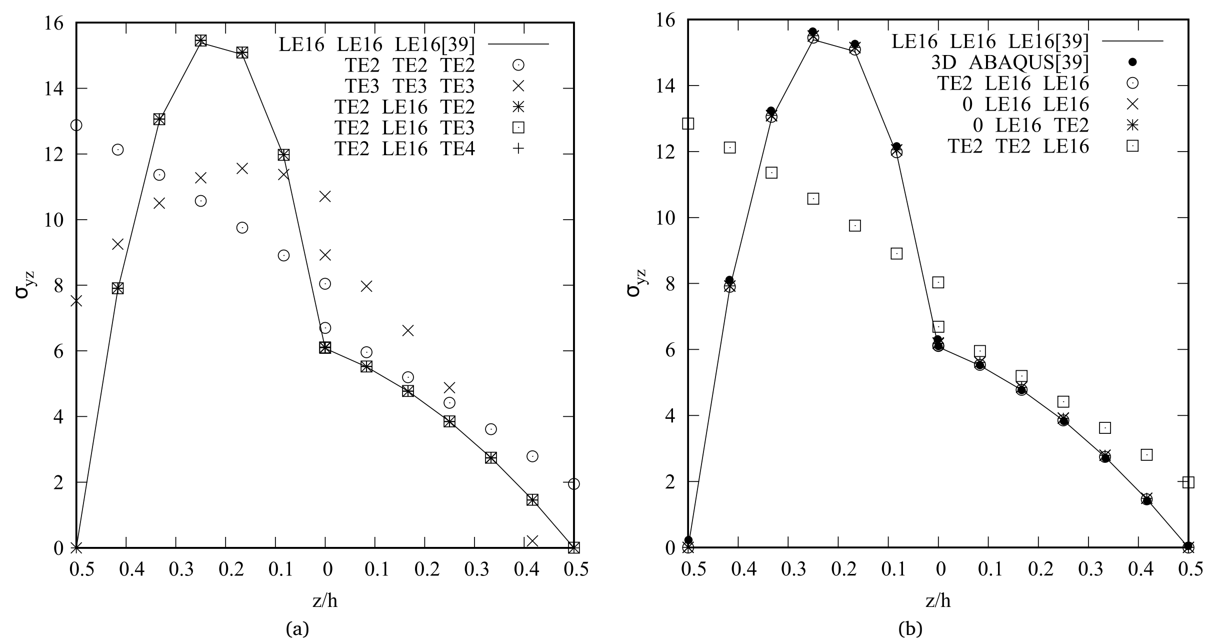

Fig. 11. Two-layer cross-ply beam subjected to bending. Shear stresses, σ_{yz}, calculated in $[0, L/2, z]$ for the reference and the present models. Linear analysis.

the total number of terms M_{u_l}. The first rows illustrate the reference solution LE16-LE16-LE16 and the uniform Taylor models. Finally, the information of several mixed ESL/LW models is explained. In all theories, the axial displacement u_y is modelled by the LW expansion LE16. u_x is either represented using a second-order model or entirely omitted. Several expansions are utilized to approximate the out-of-plane displacement variable u_z.

Fig. 10 presents the equilibrium curves, where the transverse displacements are evaluated as a function of the bending load. Additionally, the linear solution for the complete LE16 model is included for completeness. Then, the shear stresses for three different points of the equilibrium curve, in particular for the linear case (see Fig. 11) and when the loads are equal to $p_0 = 3 \times 10^6$ [Pa] and $p_0 = 9 \times 10^6$ [Pa]; see Figs. 12 and 13, respectively.

Based on the present results, the following key observations can be made:

- For the calculation of the equilibrium curve in Fig. 10, specifically the transverse displacement at the tip of the beam, all models accurately match the best CUF solution, i.e., LE16-LE16-LE16.

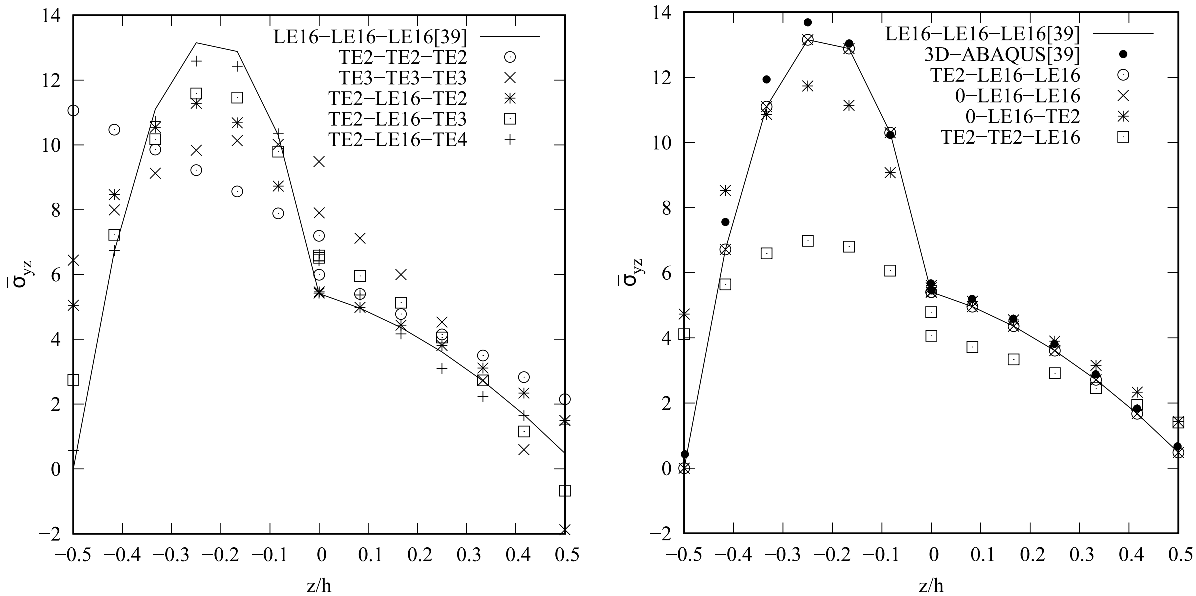

(a) (b)

Fig. 12. Two-layer cross-ply beam subjected to bending. Shear stresses, σ_{yz}, calculated in $[0, L/2, z]$ for the reference and the present models. Nonlinear analysis, $p_0 = 3 \times 10^6$ [Pa].

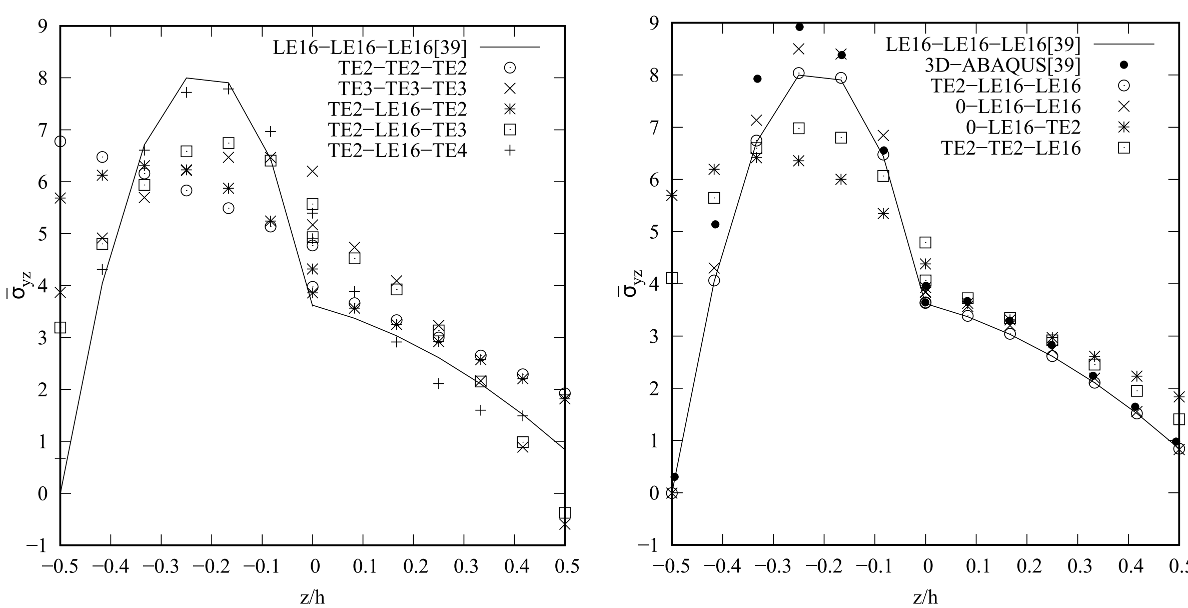

(a) (b)

Fig. 13. Two-layer cross-ply beam subjected to bending. Shear stresses, σ_{yz}, calculated in $[0, L/2, z]$ for the reference and the present models. Nonlinear analysis, $p_0 = 9 \times 10^6$ [Pa].

The most efficient model for this evaluation is TE2-LE16-TE2. Additionally, the results confirm the necessity of employing a nonlinear formulation. In fact, the linear assumptions are valid only up to $p_0 L^4/(E_2\, h^4) = 10$ circa.

- Considering the evaluation of stresses for the linear case shown in Fig. 11, all ESL/LW models exhibit the same trend as the LE16-LE16-LE16 and the 3D-ABAQUS models except TE2-TE2-LE16, since the u_y displacement component has to be described by the LW approach. On the other hand, the ESL models, i.e., TE2-TE2-TE2 and TE3-TE3-TE3, do not follow the correct trend.
- However, in the nonlinear regime, the stress predictions may vary across different models, as illustrated in Figs. 12 and 13. Notably, the transverse displacement variable u_z plays a crucial role, differently from the linear regime, confirming that the LW approach must be employed for accurate stress evaluation. This effect is more evident for $p_0 = 9\times10^6$ [Pa]. Also, the displacement component u_x becomes more important, even though the ESL approach is sufficient. For linear and $p_0 = 3\times10^6$, models 0-LE16-LE16 and 0-LE16-TE2 are very near to LE16-LE16-LE16, whereas it is not true at $p_0 = 3 \times 10^6$. In the nonlinear regime, some

differences arise between the best CUF models and the ABAQUS solution.
- The results indicate that the significance of the terms for each displacement variable varies depending on the equilibrium point considered. Furthermore, the dimensionless shear stresses exhibit lower peak values as the loading increases.

6. Conclusions

This paper presents a nonlinear beam framework based on the principles of the Carrera Unified Formulation (CUF). The aim of this paper arises from the need to reduce computational costs in the nonlinear analysis of composite beam structures. In the literature, highly refined models are typically required to capture complex equilibrium curves and stresses, particularly shear stresses. Another challenge is that efficient ad-hoc models usually demand re-derivation of the finite element matrices for each case, a process that is especially time-consuming in nonlinear quasi-static frameworks. To address these issues, a unified method is proposed, allowing researchers to flexibly select the desired models within a consistent framework.

Thus, a framework has been introduced to modify and extend the capabilities of CUF by allowing each displacement variable to adopt independent expansions and approaches. This method has already been applied to the linear analysis of beams, plates, and shells, yielding efficient results across various geometric configurations and boundary conditions [45–47]. In this paper, the full Green–Lagrange strain relationships are incorporated into the formulation to accurately capture out-of-plane stresses. Thus the nonlinear governing equations are derived and the associated finite element matrices are calculated. In particular, the proposed formulation employs Newton–Raphson linearization in combination with the arc-length method.

For the verification of the models, two case studies have been considered. The first focused on postbuckling behaviour, including a comparison of the corresponding computational times. Then a two-layered beam subjected to large deflections was later considered, along with a precise out-of-plane calculation.

The key conclusions drawn from this study are as follows:

- Computational costs can be significantly reduced by selectively incorporating only the most relevant terms within the structural theories.
- The choice of models depends on the desired outcome, whether displacements or stresses. Indeed, the accurate evaluation of out-of-plane stresses in multilayered structures may require higher-order models based on the LW approach.
- Integrating Taylor and Lagrange expansions within the same model serves as a powerful computational accelerator, while maintaining a good accuracy at the same time. Then, the union with reduced models are even more powerful in decreasing the DOFs.
- Furthermore, at each equilibrium point, the significance of different terms varies, requiring adjustments to the most accurate models to adapt to specific conditions. For instance, a displacement component may have no influence in the linear regime but become significant at higher load levels, as demonstrated in the second benchmark.

In conclusion, this paper has demonstrated the feasibility of developing a unified formulation within the nonlinear framework. In this approach, each displacement component can be assigned its own theory, and mixed ESL/LW models can be employed. Several capabilities of the formulation have been illustrated; however, future work should focus on systematically studying the different models and extending the analysis to thin-walled structures.

Finally, one of the main future goals is to extend the proposed nonlinear approach to the systematic study of laminated plate and shell structures by further developing the two-dimensional CUF framework. Second, it would also be of interest to incorporate thermal and electric fields into the nonlinear analysis and to investigate the relevance of reduced models and mixed ESL/LW approaches.

CRediT authorship contribution statement

E. Carrera: Writing – review & editing, Supervision, Methodology, Funding acquisition, Conceptualization. **D. Scano:** Writing – original draft, Visualization, Validation, Software, Methodology, Investigation, Formal analysis, Data curation, Conceptualization.

Declaration of competing interest

The authors declare that they have no known competing financial interests or personal relationships that could have appeared to influence the work reported in this paper.

Appendix. Explicit expression of the linear fundamental nuclei

$$\begin{aligned}K^0_{u_xu_xs\tau ji} &= \left\langle C_{11}N_jN_iF_{u_xs,x}F_{u_x\tau,x}\right\rangle + \left\langle C_{44}N_jN_iF_{u_xs,z}F_{u_x\tau,z}\right\rangle \\ &+ \left\langle C_{16}N_jN_{i,y}F_{u_xs,x}F_{u_x\tau}\right\rangle + \left\langle C_{16}N_{j,y}N_iF_{u_xs}F_{u_x\tau,x}\right\rangle \\ &+ \left\langle C_{66}N_{j,y}N_{i,y}F_{u_xs}F_{u_x\tau}\right\rangle \end{aligned}\tag{48}$$

$$\begin{aligned}K^0_{u_xu_ys\tau ji} &= \left\langle C_{12}N_jN_{i,y}F_{u_xs,x}F_{u_y\tau}\right\rangle + \left\langle C_{45}N_jN_iF_{u_xs,z}F_{u_y\tau,z}\right\rangle \\ &+ \left\langle C_{16}N_jN_iF_{u_xs,x}F_{u_y\tau,x}\right\rangle + \left\langle C_{26}N_{j,y}N_{i,y}F_{u_xs}F_{u_y\tau}\right\rangle \\ &+ \left\langle C_{66}N_{j,y}N_iF_{u_xs}F_{u_y\tau,x}\right\rangle \end{aligned}\tag{49}$$

$$\begin{aligned}K^0_{u_xu_zs\tau ji} &= \left\langle C_{13}N_jN_iF_{u_xs,x}F_{u_z\tau,z}\right\rangle + \left\langle C_{44}N_jN_iF_{u_xs,z}F_{u_z\tau,x}\right\rangle \\ &+ \left\langle C_{45}N_jN_{i,y}F_{u_xs,z}F_{u_z\tau}\right\rangle + \left\langle C_{36}N_{j,y}N_iF_{u_xs}F_{u_z\tau,z}\right\rangle \end{aligned}\tag{50}$$

$$\begin{aligned}K^0_{u_yu_xs\tau ji} &= \left\langle C_{12}N_{j,y}N_iF_{u_ys}F_{u_x\tau,x}\right\rangle + \left\langle C_{45}N_jN_iF_{u_ys,x}F_{u_x\tau,z}\right\rangle \\ &+ \left\langle C_{16}N_jN_iF_{u_ys,x}F_{u_x\tau,x}\right\rangle + \left\langle C_{26}N_{j,y}N_{i,y}F_{u_ys}F_{u_x\tau}\right\rangle \\ &+ \left\langle C_{66}N_jN_{i,y}F_{u_ys,x}F_{u_x\tau}\right\rangle \end{aligned}\tag{51}$$

$$\begin{aligned}K^0_{u_yu_ys\tau ji} &= \left\langle C_{22}N_{j,y}N_{i,y}F_{u_ys}F_{u_y\tau}\right\rangle + \left\langle C_{55}N_jN_iF_{u_ys,z}F_{u_y\tau,z}\right\rangle \\ &+ \left\langle C_{26}N_jN_{i,y}F_{u_ys,x}F_{u_y\tau}\right\rangle + \left\langle C_{26}N_{j,y}N_iF_{u_ys}F_{u_y\tau,x}\right\rangle \\ &+ \left\langle C_{66}N_jN_iF_{u_ys,x}F_{u_y\tau,x}\right\rangle \end{aligned}\tag{52}$$

$$\begin{aligned}K^0_{u_yu_zs\tau ji} &= \left\langle C_{23}N_{j,y}N_iF_{u_ys}F_{u_z\tau,z}\right\rangle + \left\langle C_{55}N_jN_{i,y}F_{u_ys,z}F_{u_z\tau}\right\rangle \\ &= \left\langle C_{45}N_jN_iF_{u_ys,z}F_{u_z\tau,x}\right\rangle + \left\langle C_{45}N_jN_iF_{u_ys,x}F_{u_z\tau,z}\right\rangle \end{aligned}\tag{53}$$

$$\begin{aligned}K^0_{u_zu_xs\tau ji} &= \left\langle C_{13}N_jN_iF_{u_zs,z}F_{u_x\tau,x}\right\rangle + \left\langle C_{44}N_jN_iF_{u_zs,x}F_{u_x\tau,z}\right\rangle \\ &+ \left\langle C_{45}N_{j,y}N_iF_{u_zs}F_{u_x\tau,z}\right\rangle + \left\langle C_{36}N_jN_{i,y}F_{u_zs,z}F_{u_x\tau}\right\rangle \end{aligned}\tag{54}$$

$$\begin{aligned}K^0_{u_zu_ys\tau ji} &= \left\langle C_{23}N_jN_{i,y}F_{u_zs,z}F_{u_y\tau}\right\rangle + \left\langle C_{55}N_{j,y}N_iF_{u_zs}F_{u_y\tau,z}\right\rangle \\ &+ \left\langle C_{45}N_jN_iF_{u_zs,x}F_{u_y\tau,z}\right\rangle + \left\langle C_{36}N_jN_iF_{u_zs,z}F_{u_y\tau,x}\right\rangle \end{aligned}\tag{55}$$

$$\begin{aligned}K^0_{u_zu_zs\tau ji} &= \left\langle C_{33}N_jN_iF_{u_zs,z}F_{u_z\tau,z}\right\rangle + \left\langle C_{55}N_{j,y}N_{i,y}F_{u_zs}F_{u_z\tau}\right\rangle \\ &+ \left\langle C_{45}N_jN_{i,y}F_{u_zs,x}F_{u_z\tau}\right\rangle + \left\langle C_{45}N_{j,y}N_iF_{u_zs}F_{u_z\tau,x}\right\rangle \\ &+ \left\langle C_{44}N_jN_iF_{u_zs,x}F_{u_z\tau,x}\right\rangle \end{aligned}\tag{56}$$

with $\langle(\ldots)\rangle = \int_V(\ldots)\mathrm{d}V = \int_V(\ldots)\mathrm{d}x\mathrm{d}y\mathrm{d}z$.

Data availability

Data will be made available on request.

References

[1] Reddy JN. Introduction to nonlinear finite element analysis with applications to heat transfer, fluid mechanics, and solid mechanics. New York, USA: Oxford University Press; 2014.

[2] Seffen KA, Pellegrino S. Deployment dynamics of tape springs. Proc R Soc Lond Ser A Math Phys Eng Sci 1999;455:1003–48.

[3] Warren PA. Foldable member. USA patent. 6:B1. 1969.

[4] Blanchard L, Aridon G, Falzon F, Remond D, Dufour R. A tape-spring hexapod for deployable telescopes: Dynamics. In: International conference on space optics—ICSO 2006. vol. 10567, SPIE; 2017, p. 306–2011.

[5] Pica G, Ciofaniello L, Mattei S, Santovito MR, Gardi R. High-resolution deployable telescope for satellite applications. In: Sensors, systems, and next-generation satellites VII. vol. 5234, SPIE; 2004, p. 531–8.

[6] Carrera E. Historical review of Zig-Zag theories for multilayered plates and shells . Appl Mech Rev 2003;56(3):287–308.

[7] Love AEH. A treatise on the mathematical theory of elasticity. Cambridge University Press; 2013.

[8] Frish-Fay R. Flexible bars. Washington D.C., USA: Buttleworth; 1962.

[9] Euler L. Methodus inveniendi lineas curvas maximi minimive proprietate gaudentes sive solutio problematis isoperimetrici latissimo sensu accepti. vol. 1, Berlin, Germany: Springer Science & Business Media; 1952.

[10] Timoshenko SP. On the transverse vibrations of bars of uniform cross section. Phil Mag 1922;43:125–31.

[11] Reissner E. On one-dimensional large-displacement finite-strain beam theory. Stud Appl Math 1973;52(2):87–95.

[12] Lanc D, Turkalj G, Pesic I. Global buckling analysis model for thin-walled composite laminated beam type structures. Compos Struct 2014;111:371–80.

[13] Kurtaran H. Geometrically nonlinear transient analysis of thick deep composite curved beams with generalized differential quadrature method. Compos Struct 2015;128:241–50.

[14] Kapania RK, Raciti S. Nonlinear vibrations of unsymmetrically laminated beams. AIAA J 1989;27(2):201–10.

[15] Obst AW, Kapania RK. Nonlinear static and transient finite element analysis of laminated beams. Compos Eng 1992;2(5):375–89, Use of Composites in Rotorcraft and Smart Structures.

[16] Özütok A, Madenci E. Static analysis of laminated composite beams based on higher-order shear deformation theory by using mixed-type finite element method. Int J Mech Sci 2017;130:234–43.

[17] Singh G, Rao G Venkateswara, Iyengar NGR. Nonlinear bending of thin and thick unsymmetrically laminated composite beams using refined finite element model. Comput Struct 1992;42(4):471–9.

[18] Chandrashekhara K, Bangera KM. Linear and geometrically non-linear analysis of composite beams under transverse loading. Compos Sci Technol 1993;47(4):339–47.

[19] Krawczyk P, Frey F, Zielinski AP. Large deflections of laminated beams with interlayer slips: Part 1: model development. Eng Comput 2007;24(1):17–32.

[20] Krawczyk P, Rebora B. Large deflections of laminated beams with interlayer slips: Part 2: finite element development. Eng Comput 2007;24(1):33–51.

[21] Vidal P, Polit O. Assessment of the refined sinus model for the non-linear analysis of composite beams. Compos Struct 2009;87(4):370–81.

[22] Mororó LAT, Melo AMC, Junior EP. Geometrically nonlinear analysis of thin-walled laminated composite beams. Lat Am J Solids Struct 2015;12(11):2094–117.

[23] Li Z-M, Qiao P. Thermal postbuckling analysis of anisotropic laminated beams with different boundary conditions resting on two-parameter elastic foundations. Eur J Mech A Solids 2015;54:30–43.

[24] Reddy JN. Mechanics of laminated composite plates and shells: theory and analysis. New York, USA: CRC Press; 1997.

[25] Machado SP. Non-linear buckling and postbuckling behavior of thin-walled beams considering shear deformation. Int J Non-Linear Mech 2008;43(5):345–65.

[26] Mohri F, Eddinari A, Damil N, Potier Ferry M. A beam finite element for non-linear analyses of thin-walled elements. Thin-Walled Struct 2008;46(7):981–90, A special issue to mark the Retiral of Professor Jim Rhodes, Founding Editor.

[27] Xie F, Qu Y, Zhang W, Peng Z, Meng G. Nonlinear aerothermoelastic analysis of composite laminated panels using a general higher-order shear deformation zig-zag theory. Int J Mech Sci 2019;150:226–37.

[28] Khaniki HB, Ghayesh MH, Chin R, Hussain S. Nonlinear continuum mechanics of thick hyperelastic sandwich beams using various shear deformable beam theories. Contin Mech Thermodyn 2022;34(3):781–827.

[29] Kim H-J, Yoon K, Lee P-S. Continuum mechanics based beam elements for linear and nonlinear analyses of multi-layered composite beams with interlayer slips. Compos Struct 2020;235:111740.

[30] Adam C, Ladurner D, Furtmueller T. Moderately large deflection of slightly curved layered beams with interlayer slip. Arch Appl Mech 2022;92:1431–50.

[31] Pagani A, Carrera E, Augello R, Scano D. Use of Lagrange polynomials to build refined theories for laminated beams, plates and shells. Compos Struct 2021;276.

[32] Carrera E, Cinefra M, Petrolo M, Zappino E. Finite element analysis of structures through unified formulation. John Wiley & Sons; 2014.

[33] Carrera E, Giunta G. Refined beam theories based on a unified formulation. Int J Appl Mech 2010;02(01):117–43.

[34] Carrera E, Giunta G, Nali P, Petrolo M. Refined beam elements with arbitrary cross-section geometries. Comput Struct 2010;88(5):283–93.

[35] Carrera E, Giunta G, Petrolo M. A modern and compact way to formulate classical and advanced beam theories. Dev Comput Struct Technol 2010;75–112.

[36] Carrera E, Petrolo M. Refined beam elements with only displacement variables and plate/shell capabilities. Meccanica 2012;47:537–56.

[37] Carrera E, Augello R, Scano D. Multilayered beam, plate and shell theories with interlaminar variables and Lagrange polynomials. Mem Dell'Accademia Delle Sci di Torino 2022;99–134.

[38] Pagani A, Carrera E. Unified formulation of geometrically nonlinear refined beam theories. Mech Adv Mater Struct 2018;25(1):15–31.

[39] Pagani A, Carrera E. Large-deflection and post-buckling analyses of laminated composite beams by carrera unified formulation. Compos Struct 2017;170:40–52.

[40] Pagani A, Augello R, Carrera E. Frequency and mode change in the large deflection and post-buckling of compact and thin-walled beams. J Sound Vib 2018;432:88–104.

[41] Pagani A, Carrera E. Unified one-dimensional finite element for the analysis of hyperelastic soft materials and structures. Mech Adv Mater Struct 2023;30(2):342–55.

[42] Pagani A, Daneshkhah E, Xu X, Carrera E. Evaluation of geometrically nonlinear terms in the large-deflection and post-buckling analysis of isotropic rectangular plates. Int J Non-Linear Mech 2020;121:103461.

[43] Wu B, Pagani A, Chen WQ, Carrera E. Geometrically nonlinear refined shell theories by carrera unified formulation. Mech Adv Mater Struct 2021;28(16):1721–41.

[44] Schardt R. Eine erweiterung der technischen biegetheorie zur berechnung prismatischer faltwerke. Der Stahlbau 1966;35:161–71.

[45] Carrera E, Scano D. Beam finite element models with node dependent kinematics and arbitrary displacement fields over the cross-section. Mech Adv Mater Struct 2025.

[46] Carrera E, Scano D, Zappino E. Plate finite elements with arbitrary displacement fields along the thickness. Finite Elem Anal Des 2025;244:104296.

[47] Carrera E, Scano D. Complete variable kinematics CUF-based multilayered shell elements. In: 16th world congress on computational mechanics and 4th pan American congress on computational mechanics. 2024.

[48] Bathe KJ. Finite element procedure. Upper Saddle River, New Jersey, USA: Prentice hall; 1996.

[49] Crisfield MA. Non-linear finite element analysis of solids and structures. Chichester, West Sussex, UK: Wiley; 1996.

[50] Zienkiewicz OC, Taylor RL. The finite element method for solid and structural mechanics. Washington, USA: Butterworth-Heinemann; 2005.